

Copyright © 2001, by the author(s).
All rights reserved.

Permission to make digital or hard copies of all or part of this work for personal or classroom use is granted without fee provided that copies are not made or distributed for profit or commercial advantage and that copies bear this notice and the full citation on the first page. To copy otherwise, to republish, to post on servers or to redistribute to lists, requires prior specific permission.

**FULL PROFILE CHEMICAL MECHANICAL
POLISHING (CMP) METROLOGY**

by

Runzi Chang

Memorandum No. UCB/ERL M01/23

18 May 2001

Cover

**FULL PROFILE CHEMICAL MECHANICAL
POLISHING (CMP) METROLOGY**

by

Runzi Chang

Memorandum No. UCB/ERL M01/23

18 May 2001

ELECTRONICS RESEARCH LABORATORY

College of Engineering
University of California, Berkeley
94720

Full Profile Chemical Mechanical Polishing (CMP) Metrology

Runzi Chang

Research Project

Submitted to the Department of Electrical Engineering and Computer Sciences,
University of California at Berkeley, in partial satisfaction of the requirements for the
degree of **Master of Science, Plan II.**

Approval for the Report and Comprehensive Examination:

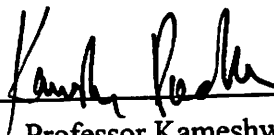
Committee:



Professor Costas J. Spanos
Research Advisor

5/25/01

(Date)



Professor Kameshwar Poolla
Second Reader

5/25/01

(Date)

CHAPTER 1	2
INTRODUCTION	2
1.1 MOTIVATION	2
1.2 REPORT ORGANIZATION	4
CHAPTER 2	5
BACKGROUND	5
2.1 BACKGROUND OF CHEMICAL MECHANICAL PLANARIZATION	5
2.2 BACKGROUND OF CMP METROLOGY	7
2.2.1 Spectroscopic Reflectometry.....	7
2.2.2 Thin Film Ellipsometry	8
2.2.3 SEM	10
2.2.4 AFM	12
2.2.5 Scatterometry.....	12
2.2.6 Monitoring CMP Processes in a Production Environment	13
2.3 BACKGROUND OF CMP PROCESS MODELING.....	14
CHAPTER 3	21
CHARACTERIZATION OF THE PATTERN DENSITY DEPENDENCY	21
3.1 INTRODUCTION	21
3.2 PROCESS SEQUENCE FOR SAMPLE PREPARATION	23
3.3 EXPERIMENTS	25
3.4 METROLOGY.....	26
3.5 DATA ANALYSIS	26
CHAPTER 4	32
ENABLING FULL-PROFILE CMP METROLOGY USING SCATTEROMETRY	32
4.1 MASK DESIGN	32
4.2 KEY IDEAS.....	34
4.3 FABRICATION ISSUES	35
4.3 PREPARATION FOR THE EXPERIMENT	36
4.4 EXPERIMENTS	38
4.5 MEASUREMENTS.....	40
4.6 FACTORIAL DATA ANALYSIS	43
4.7 A LIBRARY-BASED METROLOGY FOR MONITORING CMP PROFILE EVOLUTION	47
CHAPTER 5	54
CONCLUSIONS AND FUTURE WORK	54
5.1 REPORT SUMMARY	54
5.2 FUTURE WORK	55
REFERENCES	56

Chapter 1

Introduction

1.1 Motivation

Chemical mechanical polishing (CMP) is currently being used in the fabrication of state of the art integrated circuits, and has been identified as an enabling technology for the semiconductor industry in its drive toward gigabit chips and sub-180nm feature sizes. At the present time, it appears that the global planarization necessary for establishing reliable multilevel interconnects can only be achieved by using CMP. As with many processes that stand in the critical path of IC development, this technology has moved into production without the benefit of a complete, first principle model. In the long run, the availability of such models will help optimize the operation of CMP and permit the users to define the best operating conditions for each specific application.

This project concerns the development of a fundamental understanding of the material removal mechanism during inter-layer dielectric (ILD) CMP, in both the feature-scale and wafer-scale level. In the long term, this research will facilitate CMP technology development in at least two aspects:

- (1) It will aid in identifying the dominant relationships between the material and process parameters and the effectiveness (measured by quality and

integrity of the finished surface) and efficiency (measured by material removal rate) of a CMP process. Such a model will facilitate process optimization

- (2) In addition to providing a more fundamental understanding of the CMP process, the value of the proposed experimental and modeling efforts lies in its enhanced capability for exploration of the "design space." Currently, many process design options (e.g., optimum selection of slurry and pad properties) remain a trial-and-error proposition due to lack of reliable models depicting those effects. The proposed model will aid in identifying such unexplored process parameters and guide us toward new and novel avenues for designing CMP processes.

To achieve the above objectives, we will utilize a combination of experiments and analytical efforts. The first phase of this ambitious project is to investigate the feasibility of developing a non-destructive, low-cost metrology method to monitor the profile evolution during the ILD CMP process. In this report, I will explore the possibility of monitoring ILD CMP profile evolution using scatterometry. It is note worthy that metrology by itself in CMP is very important to the entire micro-fabrication process. Improved metrology will help us understand the process and improve the yield.

1.2 Report Organization

This report begins by providing a review of chemical mechanical polishing metrology and modeling. Different metrology candidates will be compared and the concept of scatterometry will be reviewed.

Chapter 2 provides an overview of CMP and its application.

Chapter 3 introduces the primary characterization experiments carried out in preparation of the new mask design. Important parameters were extracted and the pattern density model was validated.

Chapter 4 describes the CMP metrology and modeling experiments conducted, including design of mask and design of experiments. The measurements and results of these experiments will be discussed. More importantly, a library-based CMP profile metrology using scatterometry will be proposed and verified.

The report concludes with Chapter 5, which summarizes the results from experiments as well as offers a methodology of monitoring CMP profile evolution using scatterometry. Finally, future work related to this research is also discussed. The main work will be focusing on CMP process modeling and computer-aided CMP process design based on the results in the previous experiments.

Chapter 2

Background

Chemical Mechanical Planarization (CMP) is a process used to planarize silicon integrated circuits in-between critical patterning and deposition steps

2.1 Background of Chemical Mechanical Planarization

Rapid device scaling has been the factor governing the growth of the semiconductor industry, which has produced devices with ever-better performance characteristics in terms of high speed and low power. The semiconductor industry has been experiencing an average growth rate of 15% annually over the past three and a half decades [1]. With this fast growth has come a reduction in average cycle time between introductions of new technologies from the traditional 3-year cycle towards an approximate 2-year cycle. Current (2001) production is being done employing 0.15 μm technology, with 0.13 μm technology expected to be introduced in the year 2002. Advances in integrated circuit (IC) manufacturing have also increased device density to about 200 million transistors per cm^2 of chip area (for memory). The corresponding increase in circuit functionality requires increased levels of metal interconnect to facilitate device and module communication. Up to seven levels of metal interconnect

have been reported to date, and the experts predict a ten level interconnect by the year 2011 [2]. Figure 1 shows a typical chip cross section.

While critical dimensions (CD) continue to shrink, modern photolithography equipment approaches its depth of focus limits. Slight irregularities on

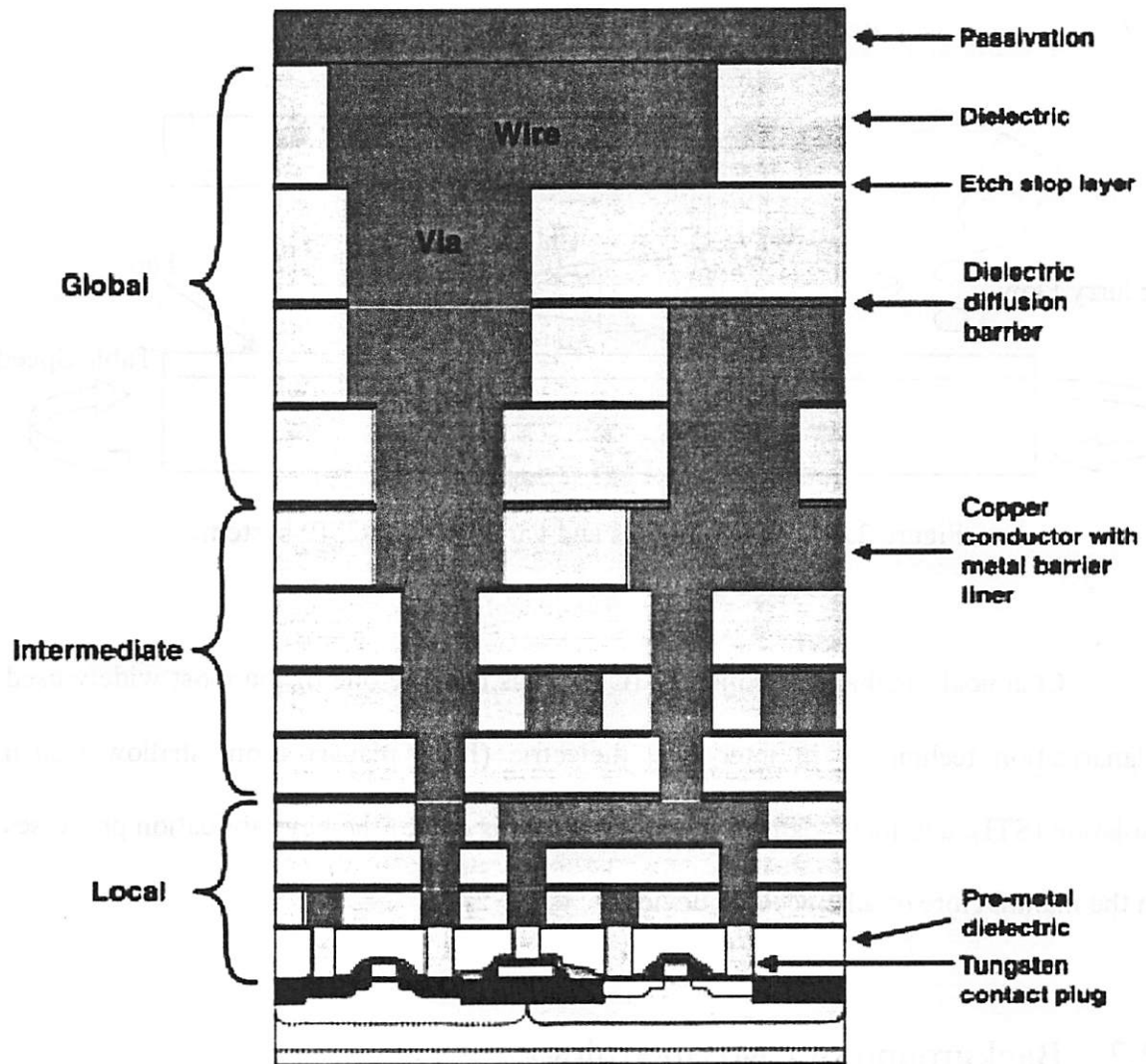


Figure 2.1 A typical chip cross section

the wafer surface—or on deposited films—can distort semiconductor patterns as they are transferred by a lithographic process to the wafer surface. Chemical mechanical planarization (CMP) has become the process of choice for preventing distortion, simply

by planarizing the wafer surface to a flat, uniform finish. To planarize the wafer, CMP systems use an abrasive suspended in a chemical slurry that levels wafer topography. Figure 2.2 shows the component in a simple CMP system.

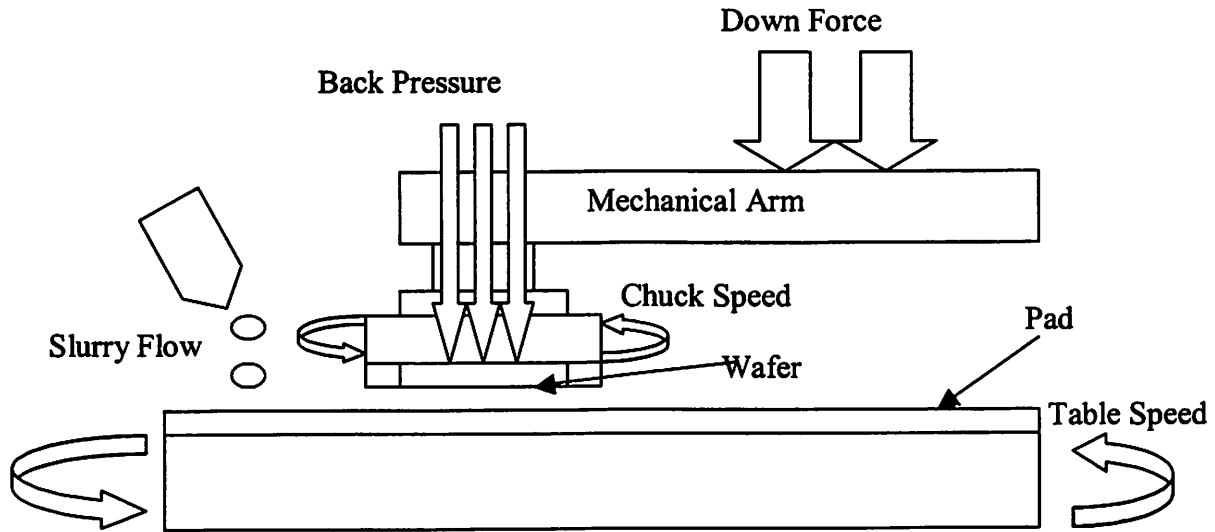


Figure 2.2 Components and variables in a CMP system

Chemical Mechanical Polishing (CMP) has become one of the most widely used planarization techniques in inter-level dielectric (ILD) planarization, shallow trench isolation (STI), and metal damascene processes. It is one of the key fabrication processes in the manufacture of advanced IC devices.

2.2 Background of CMP metrology

In this section, I will introduce several types of metrology tools that are widely used in either research or the industry.

2.2.1 Spectroscopic Reflectometry

In spectroscopic reflectometry, the reflected light intensities are measured in a broadband wavelength range. In most setups, non-polarized light is used at normal incidence. The biggest advantage of spectroscopic reflectometry is its simplicity and low cost. Figure 2.3 shows the setup of conventional spectroscopic reflectometry.

In reflectometry, only light intensities are measured. The relation between the *reflectance* R and the complex *reflection coefficient* r is $R = |r|^2$.

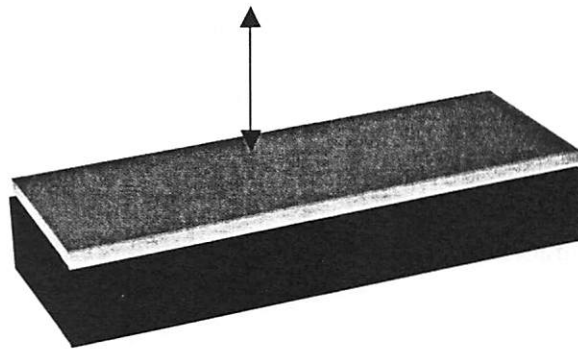


Figure 2.3 Spectroscopic reflectometry measurements.

This method is simple and easy for implementation. I will introduce its real application in section 2.2.5 and discuss its advantages and constraints then.

2.2.2 Spectroscopic Ellipsometry

Ellipsometry has become an integral part of the metrology system employed in the semiconductor industry. This method is based on the characteristics of light upon reflection from a surface. The component waves of light, which are linearly polarized with the electric field vibrating parallel (p or TM) or perpendicular (s or TE) to the plane of incidence, behave differently upon reflection. The component waves experience

different amplitude attenuations as well as different absolute phase shifts upon reflection; as such, the overall state of polarization changes. Ellipsometry refers to the measurement of the state of polarization before and after reflection for the purpose of determining the properties of the reflecting boundary. The measurement is usually expressed in the form

$$\rho = \tan\Psi e^{j\Delta} = \frac{r_p}{r_s},$$

where r_p and r_s are the complex reflection coefficients for TM and TE waves respectively.

Ellipsometry derives its increased sensitivity over reflectometry from the fact that the polarization-altering properties of the reflecting boundary are modified significantly even when ultra-thin films are present. Consequently, Ellipsometry has become the rigorous method of characterizing thin films. An illustration of the basics of ellipsometry is presented in Figure 2.4 below:

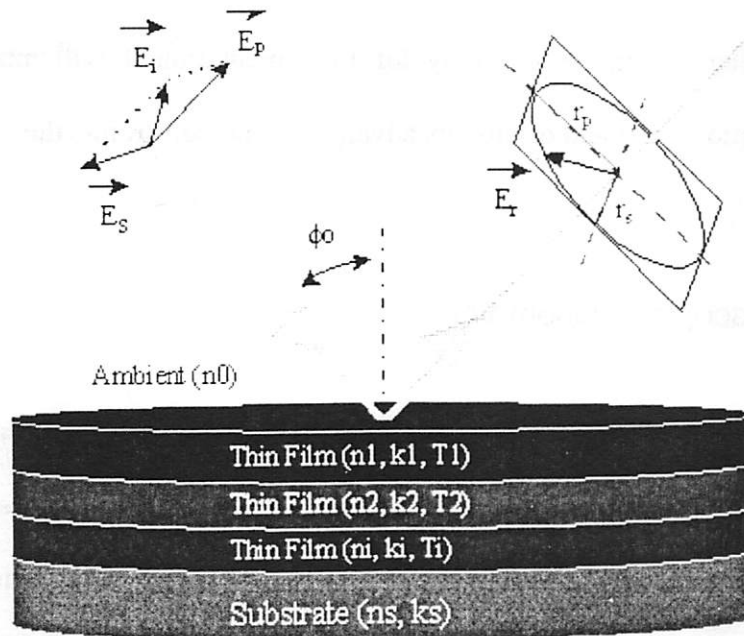


Figure 2.4 Spectroscopic Ellipsometry Measurements

Ellipsometry analyzes the polarization-state-in and polarization-state-out of light incident on a thin film. Typically light with wavelength in the visible range is used; however, virtually any polarizable wave can be used to produce an ellipsometric measurement.

The advantage of ellipsometry over reflectometry is its accuracy. Firstly, ellipsometry measures the polarization state of light by looking at the ratio of values rather than the absolute intensity of the reflected light. This property is especially useful in the DUV wavelength range, where very little light is typically available. Second, ellipsometry can gather the phase information in addition to plain magnitude reflectivity information. Phase information provides more sensitivity to thin-film variations.

2.2.3 Scanning Electron Microscopy (SEM)

The scanning electron microscope (SEM) is currently the workhorse instrument used in production for measuring sub-micron features because of its nanometer-scale resolution, precision as well as high throughput. The SEM is divided into two types: cross-sectional and top-down.

Cross-sectional SEM can provide profile information for structures on a wafer in the form of a direct image. This image can be used immediately for process characterization. However, obtaining a cross-sectional SEM image requires breaking a wafer and is very time-consuming, also there is the possibility of the presence of systematic profile errors dependent upon the image processing technique being employed.

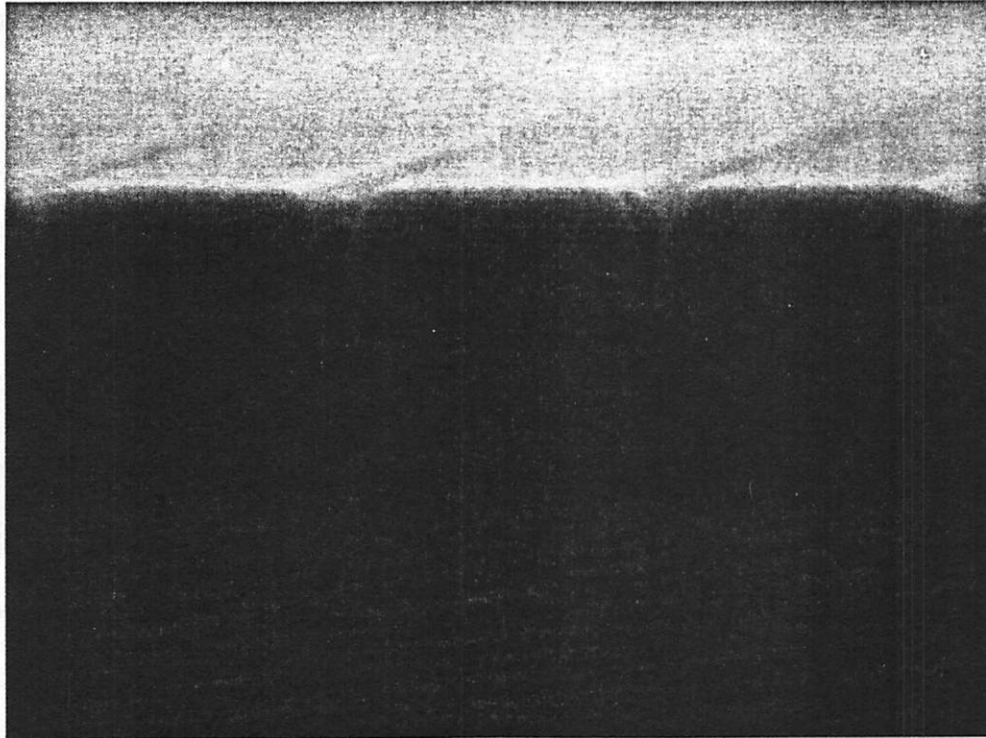


Figure 2.5 A cross-sectional view of a sample using SEM

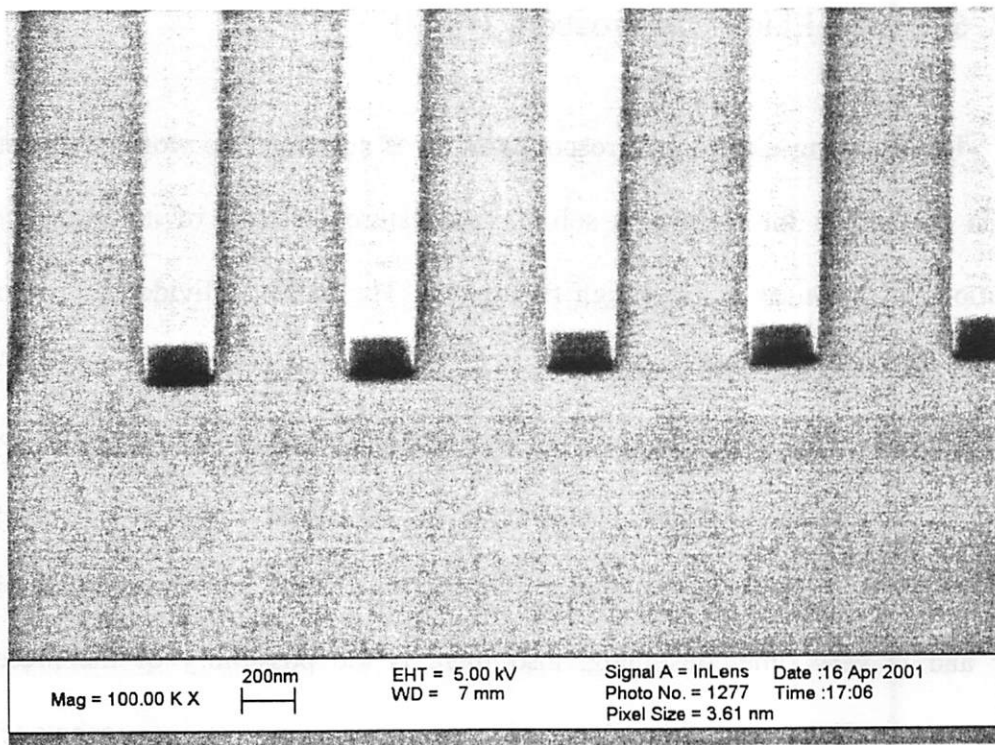


Figure 2.6 A top-down view of a E-beam Lithography sample using SEM

The top-down SEM, more commonly referred to as the CD-SEM, measures the CD of a profile at a somewhat arbitrary height and does not take into account the slope associated with the profile that results in a constantly changing profile CD. Another problem associated with this method is the build-up of charge in the sample under the electron beam. The CD-SEM, being a surface scanning technique, is also unable to provide information on underlying layers of the structure as well as undercut features. The state-of-the-art SEMs can measure CDs with a precision of about 2nm.

2.2.4 Atomic Force Microscopy (AFM)

Atomic force microscopy (AFM) provides a resolution between 0.1nm and 5nm, depending on the hardness of the material being scanned. For typical semiconductor profiles, this translates into exceptionally high vertical and lateral resolutions, which combine to provide information about a patterned structure's width, sidewall slope and thickness. However, current AFM scan rates are very slow, and measurement accuracy and precision are highly dependent upon the tip shape and stability. At present, the AFM is too slow to be used for real-time imaging or in-line measurements during a CMP process.

2.2.5 Scatterometry

Scatterometry is the metrology that relates the geometry of a sample to its light scattering effects. In the same way that ellipsometry analyzes polarization-state-in and

polarization-state-out of light incident on thin film, scatterometry adopts the same theory and measures the polarization-state-in and polarization-state-out of light, incident not on a thin film, but rather on periodic surface structures. The $\tan \Psi$ and $\cos \Delta$ values are measured after reflection and matched to the responses of known profiles.

Much work has been done on scatterometry in recent years. McNeil et al have explored the idea of variable-angle scatterometry, which uses angle-resolved diffracted light analysis to measure etched samples with line width dimensions as small as 150nm and poly-Si thickness on the order of 250nm [3].

Niu et al. have explored the idea of spectroscopic scatterometry, in which the responses for multiple wavelengths are taken into account [4]. This method consists of measurements taken at a fixed incident angle as opposed to variable-angle scatterometry. The lack of external moving parts, and hence simpler implementation, gives spectroscopic scatterometry the potential of being employed in in-line, in-situ process control. Niu et al also developed a simulation engine, known as the gtk (Grating Tool Kit) based on the Rigorous Couple-Wave Analysis [5-6]. It was demonstrated that the simulated and measured diffracted light responses based on this technique correspond with profiles that closely match those obtained through the AFM.

2.2.6 Monitoring CMP Processes in a Production Environment

Accurate thickness measurements in chemical mechanical polishing (CMP) are difficult to achieve consistently on complex state-of-the-art computer chips, so frequent monitoring is needed. This requires high-speed film thickness measurement of both thick

films and ultra-thin films at multiple sites across the wafer surface. In order to make film removal uniformity measurements on product wafers, the metrology tool must have a small measurement spot and fast, robust pattern recognition to reliably guide the measurement spot to the film thickness test structures.

Spectroscopic reflectometers have been used to measure thick films because they can determine film thickness very rapidly. They also can operate with measurement spots as small as $\sim 50\mu\text{m}$ in diameter. However, reflectometer accuracy degrades significantly when measuring films thinner than 500-1,000 Å. The ability to measure very thin films is important in determining if over-polishing has occurred. On the other hand, measurement accuracy and reliability for thick films are challenging qualities in a production CMP metrology system. Inaccurate measurements resulting from the phenomenon known as "order skipping" for instance, lead to mis-processing and costly scrapping of damaged wafers.

Metrology methods which can overcome the slow throughput and meet the requirements of state-of-the-art CMP process-control are needed. For research purposes, metrology methods which can monitor the profile evolution would be crucial for the development and verification of a rigorous, first principal model for the state-of-the-art CMP process.

2.3 Background of CMP process modeling

The main feature of CMP, namely the removal of the material, is described by the Preston's Equation [7]:

$$\frac{dT}{dt} = K \cdot \frac{N}{A} \cdot \frac{ds}{dt}$$

where T denotes the thickness of the wafer, N/A denotes the pressure caused by the normal force N on the area A. s is the total distance traveled by the wafer, and t denotes the elapsed time. This means that the material removal rate is proportional to the pressure and the velocity of the rotation. Any physical considerations are put into the Preston's Constant K, which is often considered the proportionality constant (i.e. independent of pressure and velocity), but may also contain chemical effects. However, the chemical reaction effects seem to dominate in real-life situations.

Cook's model [8] is applicable to CMP for bare silicon wafers. However, many ideas are also applicable to the more general case of CMP for ILD. He starts from Preston's Equation. The slurry is assumed to be a viscous Newtonian fluid with a viscosity of around 10⁹P with particles in it. The mechanical part of the interaction between polishing particles and the wafer surface can be described by a model with a spherical particle of diameter Φ , which penetrates the surface with force F_s under the uniform load N. For a standard Hertzian penetration Preston's constant becomes $(2 \cdot E)^{-1}$, where the E denotes Young's modulus. The surface roughness is the penetration depth given by

$$R_s = \frac{3}{4} \cdot \Phi \cdot \left(\frac{P}{2 \cdot k \cdot E} \right)^{2/3}$$

where k is the particle concentration (unity for a fully-filled closed packing) and $P = \frac{N}{A}$ is the pressure.

Impingement of particles carried in the turbulent liquid leads to Hertzian penetration of the surface, converting kinetic energy into strain energy. Local bonding during contact leads to weakening of binding forces at the surface, which allows atomic removal to occur without introducing lattice dislocations.

An extensive study of the chemical part is presented in Cook's paper. However, a discussion of it is beyond the scope of this report.

Cook's model is the most elaborate modeling work for polishing so far. In particular, it deals with the mechanics of the polishing particles and with the chemical reactions. It covers almost all interesting topics and the method is explained by an example (SiO₂ polished by SiO₂-particles). This model is based on a smaller feature length compared to the Preston's model, as it deals with the particles and the particle size in the slurry fluid. In the future, additional work is necessary to combine Cook's model with other models in order to get a sufficiently general model for the entire CMP process.

J. Luo and D.A. Dornfeld at the university of California, Berkeley have explored the material removal mechanism in chemical mechanical polishing recently [9]. Based on the assumptions of plastic contact over wafer–abrasive and pad–abrasive interfaces, the normal distribution of abrasive size and the periodic roughness of the pad surface, a novel model was developed for predicting the material removal in CMP. The basic idea of the model is that $MRR = \rho_w N \cdot Vol_{removed}$, where ρ_w is the density of the wafer, N the number of active abrasives and $Vol_{removed}$ is the volume removed by a single abrasive.

Compared with previous modeling approaches, such as Preston's equation, the model proposed by Luo and Dornfeld integrates not only the process parameters of pressure and velocity, but also other input parameters including the wafer hardness, pad hardness, pad roughness, abrasive size and abrasive geometry into the same formulation to predict the material removal rate. An interface between the chemical effect and mechanical effect has been constructed through a fitting parameter in the model. It reflects the influence of chemicals on the mechanical material removal. The fluid effect in the current model is attributed to the number of active abrasives. The nonlinear down pressure dependence of material removal rate is related to a probability density function of the abrasive size and the elastic deformation of the pad. Compared with experimental results, the proposed model predicts the material removal rate fairly accurately.

At this point it is appropriate to mention the MIT work on pattern dependency effects [10-11]. Several models had been proposed to account for pattern effects in CMP before the MIT Model but their applicability had been limited [12]. The limitations ranged from being based on non-representative test structures to probing of small process windows which limit the utility of the models beyond the scope of the original experimental conditions. Most of the models before the MIT model, however, did not apply across a whole die but rather focused on individual features.

As a prelude to effective modeling of CMP for oxide planarization, the MIT metrology group performed polishing experiments for a wide range of die topography patterns. A set of four masks shown in Figure 2.7 was used to generate the die patterns. Mask I explores the effects of area and consists of blocks of sizes ranging from 20 μm to 3000 μm . It also contains blocks which mimic realistic circuit layouts. Mask II examines

the effect of pitch. The pattern density – defined as the ratio of line width to pitch – is maintained at 50% while the pitch is varied from $2\mu\text{m}$ to $1000\mu\text{m}$ in the $2\text{mm} \times 2\text{mm}$ blocks. Mask III explores the effect of density which is increased from 4% to 100% in steps of 4%. Pitch is maintained at $250\mu\text{m}$ in each of the 25 $2\text{mm} \times 2\text{mm}$ blocks. Mask IV explores the effects of block perimeter. It consists of blocks of constant area ($1\text{mm} \times 1\text{mm}$) but with different perimeter/area ratios. The mask is divided into six sections and the spaces between the blocks are decreased from $60\mu\text{m}$ at the bottom to $10\mu\text{m}$ at the top.

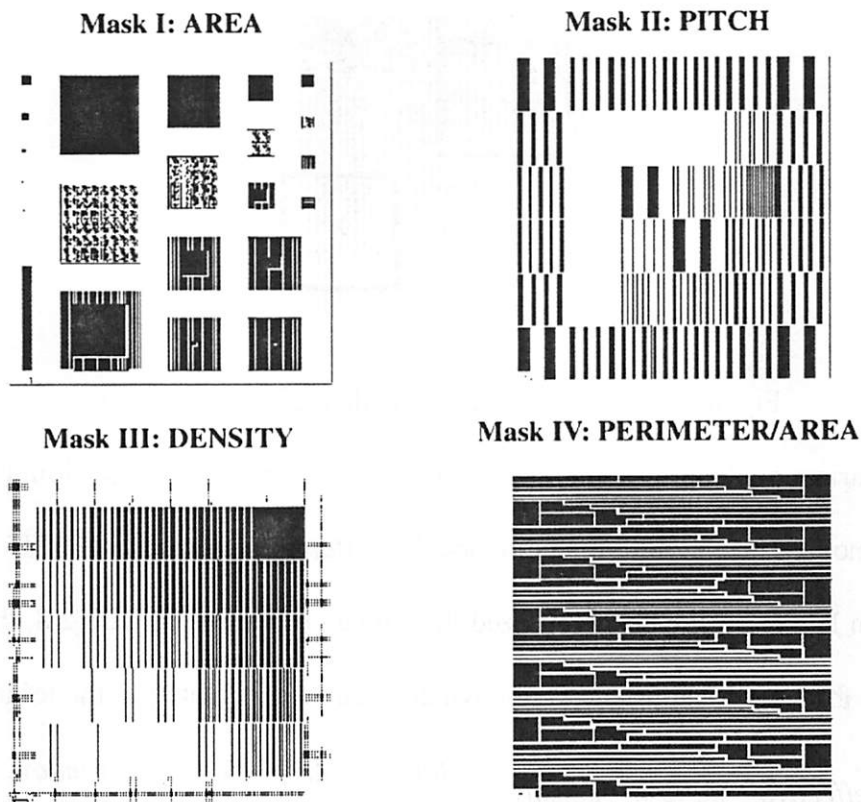


Figure 2.7 MIT oxide CMP characterization mask set

These masks were used in a single-mask fabrication process to generate surface topographies on 6" wafers to be planarized using CMP. The fabrication process consisted of 1000nm LPCVD TEOS deposition, metal deposition, pattern and etch followed by 2000nm TEOS deposition.

The experimental results led to two important conclusions which are becoming the basis for the later MIT CMP model: (1) the pitch (line width and line space), area and perimeter are all minor effects to the final oxide thickness; (2) effective density is the key layout parameter. That is, the oxide-polishing rate at each point is inversely proportional to the effective pattern density. The effective pattern density depends on the nearby topography and density. A certain window, whose side is so called the “planarization length”, can determine the pattern density. Please see Figure 2.8 for the illustration.

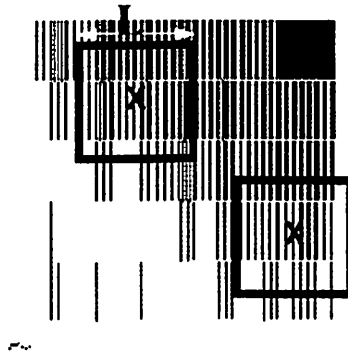


Figure 2.8 window used to calculate effective density

Planarization length is the approximate length of the “ramp” joining areas of different removal rates, as determined by locally different pattern densities. However, the planarization length must be characterized for a given process. In figure 2.8, the effective density at X for a square constant weight window can be calculated as the following:

$$\text{effective - pattern - density} = \frac{\text{Raised - Area - in - the - window}}{\text{Total - Area - in - the - window}}$$

The long range “moving average” density calculation corresponds to a simple convolution picture:

$$d(x, y) = p(x, y) * l(x, y)$$

Where $d(x, y)$ is the effective pattern density at (x, y) , $p(x, y)$ is the “planarization impulse response” (weighting function) to raised features, $l(x, y)$ is the local (feature scale) density.

Chapter 3

Characterization of the Pattern

Density Dependency

In recent years, chemical mechanical polishing (CMP) has become an increasingly important step in the Integrated Circuit (IC) fabrication. Whether it is the damascene process or planarization in Micro-Electro-Mechanical-System (MEMS) fabrication, the CMP process plays a crucial role in these applications. The recent purchase of the Strausbaugh 6EC, single wafer CMP machine by the micro fabrication laboratory at UC Berkeley offers the lab researchers a CMP process comparable to that of the industry. In this chapter we describe the experiments used to characterize the pattern density effect for this process.

3.1 Introduction

The MIT pattern density masks were designed for characterizing and modeling pattern dependent variation in CMP processes, consumables, and tools. While there is considerable research into physical modeling and understanding of pattern sensitivities, these masks were designed to enable methods for the rapid characterization, empirical

modeling, and comparison of pattern dependencies as a function of processes, consumables, or equipment options. The test masks and measurements enabled can also serve as a source of data for the calibration and validation of physical or semi-empirical modeling efforts.

In this experiment, the MIT pattern density masks have been exercised in a traditional backend interconnect process. A typical process flow consists of depositing a field oxide layer followed by metal deposition, pattern, and etch. After depositing the inter-layer dielectric (ILD) layer, the wafers are polished to achieve uniform surface heights.

In the MIT density mask, the pattern density was defined as the ratio of raised metal area in each structure to the total area of each structure. It was varied systematically from 4% to 100% from lowest in the lower left corner to greatest in the upper right corner while the pitch of each structure was fixed at 250 μm . A total of 25 structures each 4mm x 4mm are arranged in a 5x5 grid fashion. Each block size is 4mm x 4mm to better decouple interactions from neighboring structures. The die has an outside border with 10m wide lines. Figure 3.1 shows the mask structure.

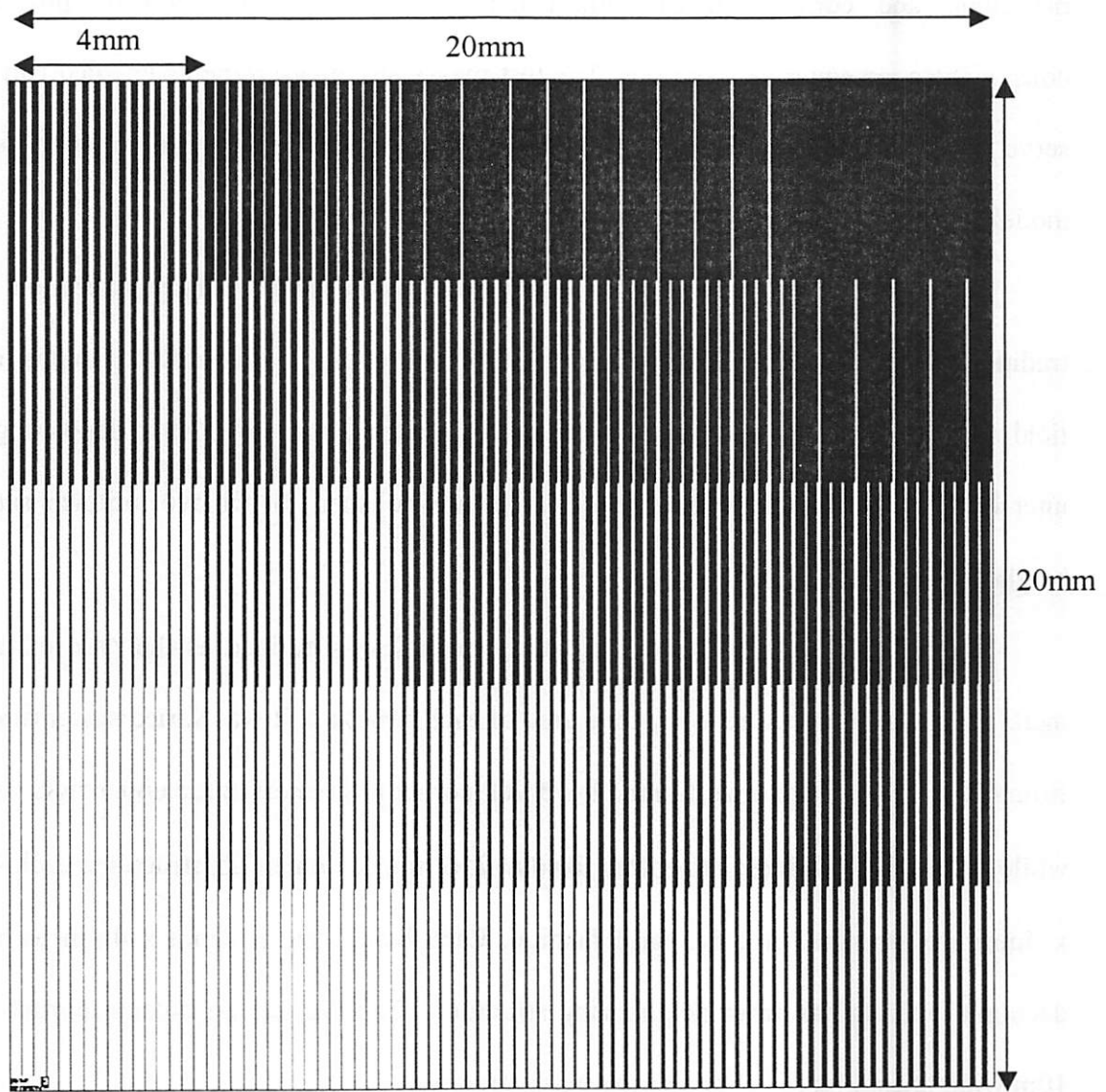


Figure 3.1 the layout of the MIT pattern density mask

3.2 Process Sequence for Sample Preparation

We started from $1\mu\text{m}$ field oxide on single crystal silicon substrate. Subsequently, using the CPA 9900 sputtering system 7000\AA Aluminum was sputtered to the surface of the wafers. Since in the micro-fabrication lab at Berkeley we did not have the ability to print 20mm die size using any of the steppers (the maximum die size was 10mm when

this experiment was done), it was decided to use the contact printing mask design in figure 3.2, which could keep the 20mm by 20mm die size, and decouple the interactions from the neighboring structures. We used 4-inch prime grade, p-type, <100>, bare silicon wafers. They were deposited with undensified PSG. Using the contact-printing mask we patterned the Aluminum film. Subsequently dry etching was performed and the exposed Aluminum was etched away in a plasma based Aluminum etcher. Finally we deposited $\sim 2.8\mu\text{m}$ oxide using LPCVD (a low temperature process operated at about 400°C). The process flow is shown in Figure 3.3.

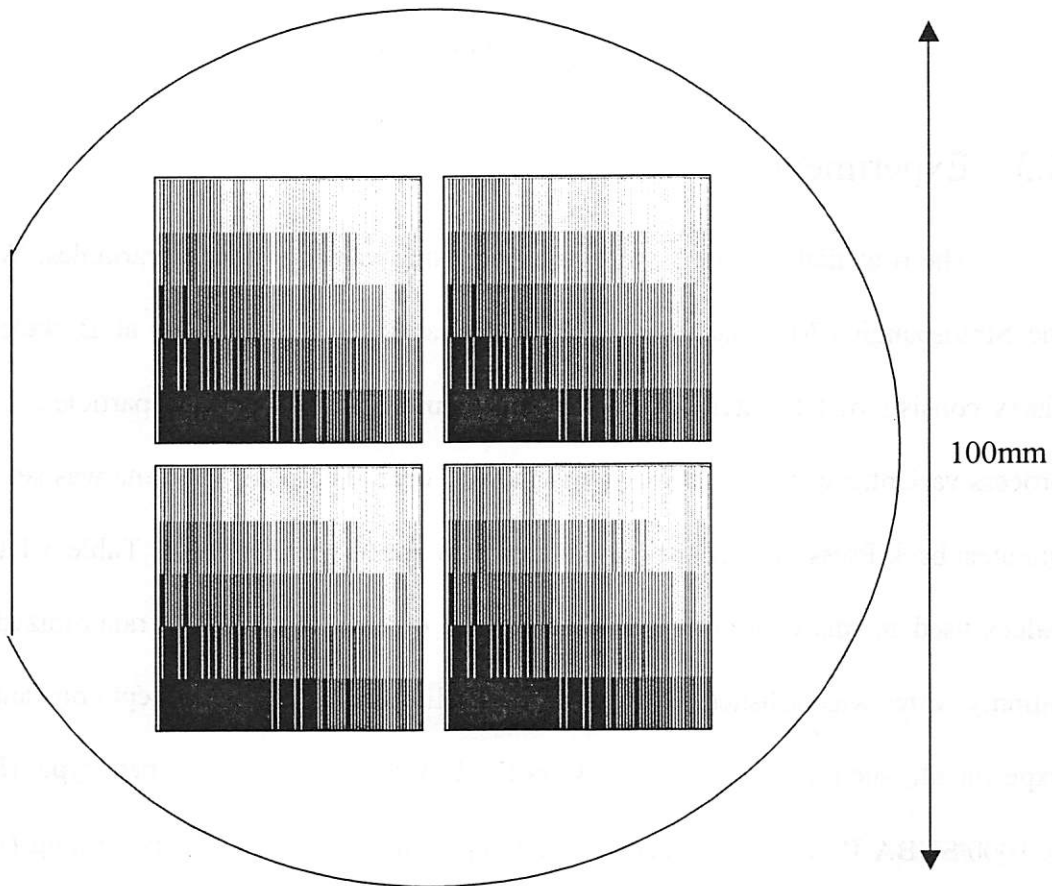


Figure 3.2 Aluminum mask used in the experiment

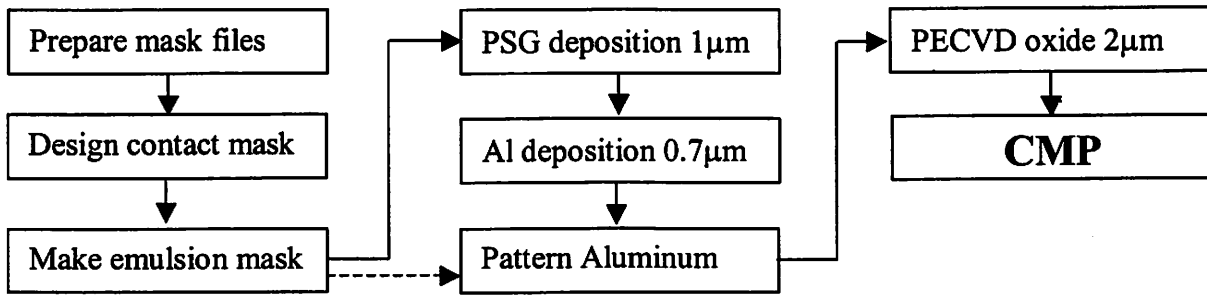


Figure 3.3 Process flow for CMP wafer fabrication

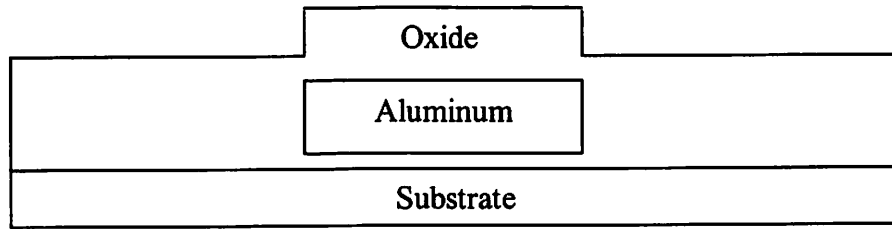


Figure 3.4 Cross section before polishing

3.3 Experiments

The 6 available wafers were polished using varying process variables. We used the Strausbaugh CMP machine in the Micro-fabrication Laboratory at Berkeley. The slurry consists of DI water, KOH, ~200nm diameter silicon dioxide particles. The two process variables were Table Speed and Down Force. The polishing time was set to be 3 minutes; back Pressure was 1psi; and slurry flow speed was 50ml/min. Table 3.1 lists the values used in this experiment. The actual run order of wafers was randomized and a dummy wafer was polished before each run. All other factors were kept constant in the experiment, such as: slurry type (Cabot's D7000 oxide slurry), pad type (Rodel's IC1000/SUBA IV composite pad), table temperature (30°C), pad conditioning (in-situ). The wafers were cleaned right after the polishing in the SSEC Evergreen CMPWC, a dedicated machine for post-CMP clean in the Micro-Lab.

Table 3.1 Experimental design for pattern density dependency characterization

Wafer #	Down Force (psi)	Table Speed (rpm)
1	5	80
2	5	120
3	7	80
4	7	120
5,6	6	100

3.4 Metrology

With generous help from Nanometrics Inc., we had access to NanoSpec 8000 FTIR: 8000XSE FTIR. Engineers in the Application Department helped develop a new recipe for Aluminum on Oxide. Semi-automated measurements were acquired before and after the CMP process. The fitting error was good except for the narrowest lines (10 μ m) since the spot size is about 16 μ m. Figure 3.5 illustrates the measurement of the sites in the whole metrology process.

3.5 Data Analysis

Sample oxide thickness data before and after polishing for wafer No.1 was listed in Table 3.2. The purpose of this experiment was to explore and verify the pattern density dependencies on our system, and also extract some important parameters in the process, such as the planarization length or the characteristic length.

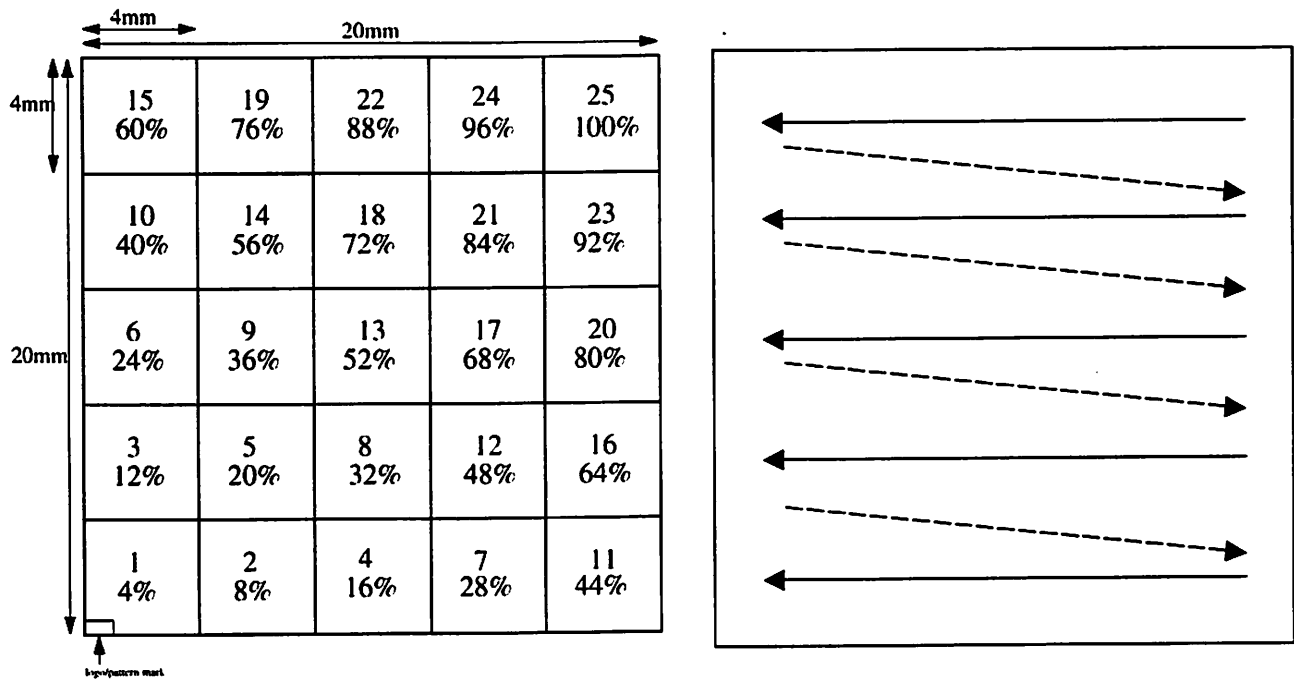
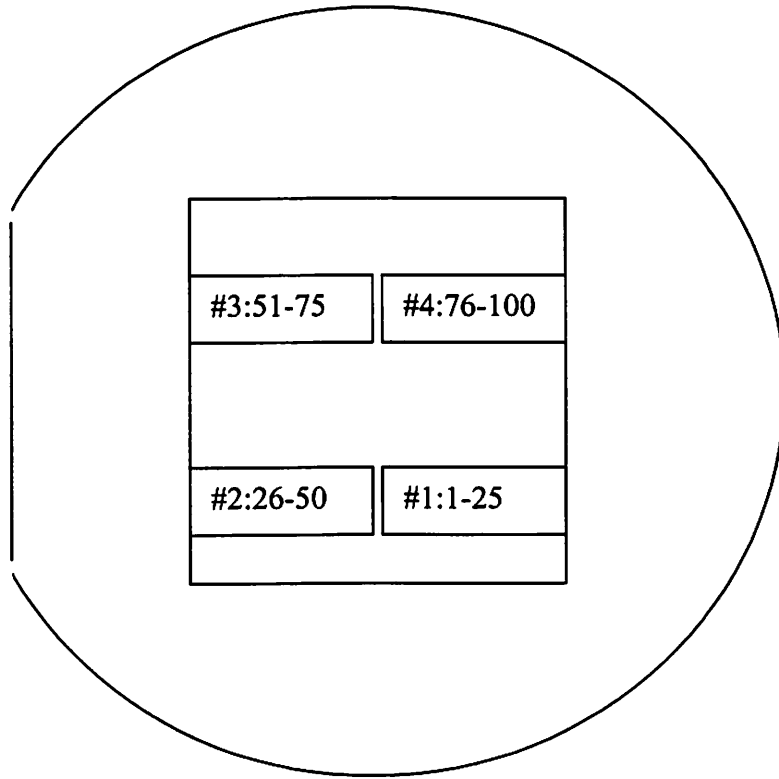


Figure 3.5 Pattern density distribution and measurement sequence

Table 3.2 ILD thickness on top of Al for wafer No.1 before and after polishing (Å)

#	before	after	#	before	after	#	before	after	#	before	after
1	28458	24939	26	28161	22258	51	28024	22624	76	28342	25408
2	28557	25254	27	28194	23141	52	28046	23496	77	28472	25794
3	28609	25079	28	28202	23516	53	28204	23805	78	28533	25635
4	28761	24649	29	28276	23496	54	28229	23874	79	28688	25206
5	28727	23782	30	28313	23209	55	28322	23991	80	28817	24337
6	28467	25243	31	28064	22609	56	27903	22516	81	28382	25262
7	28531	25412	32	28220	23284	57	28031	23248	82	28489	25406
8	28684	25085	33	28197	23451	58	28099	23363	83	28510	25100
9	28693	24550	34	28284	23322	59	28219	23308	84	28580	24514
10	28706	23491	35	28369	22948	60	28206	23177	85	28739	23312
11	28438	25113	36	28076	22192	61	27841	21688	86	28335	24563
12	28544	25112	37	28204	22811	62	27890	22207	87	28412	24505
13	28539	24608	38	28193	22740	63	28029	22065	88	28490	23927
14	28743	23840	39	28273	22514	64	28112	21886	89	28574	23008
15	28745	22743	40	28328	22377	65	28172	21536	90	28649	21547
16	28451	24754	41	27996	21581	66	27783	20202	91	28275	23410
17	28487	24660	42	28134	21878	67	27817	20451	92	28415	23067
18	28571	23856	43	28218	21717	68	27891	20240	93	28512	22076
19	28651	22983	44	28213	21487	69	27988	21694	94	28537	20776
20	28603	21606	45	28243	21134	70	28040	21057	95	28538	21123
21	28445	24216	46	27956	20576	71	27654	20125	96	28190	21445
22	28481	23739	47	28112	20740	72	27789	20000	97	28256	20731
23	28580	22750	48	28122	20351	73	27851	22483	98	28325	21445
24	28587	21183	49	28108	21761	74	27918	22187	99	28442	20047
25	28593	21746	50	28207	21178	75	28105	25215	100	28577	28183

Looking through a window whose size equals the characteristic length, the pressure is:

$$p \propto \frac{F}{A} = \frac{F}{A_0 * pattern_density}$$

where A is the actual contact area and A_0 is the nominal contact area. We expect that:

$$Material_Removal_Rate \propto \frac{1}{pattern_density}$$

simply based on the Preston's Equation. The idea of planarization length can be illustrated in Figure 3.6. This length is a function of the pad property (i.e. hardness) and also the polishing system (i.e., wafer diameter, etc).

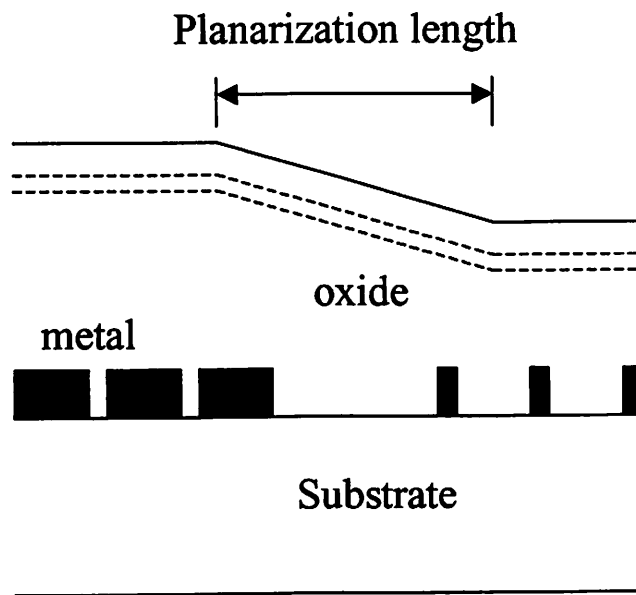


Figure 3.6 The illustration of planarization length

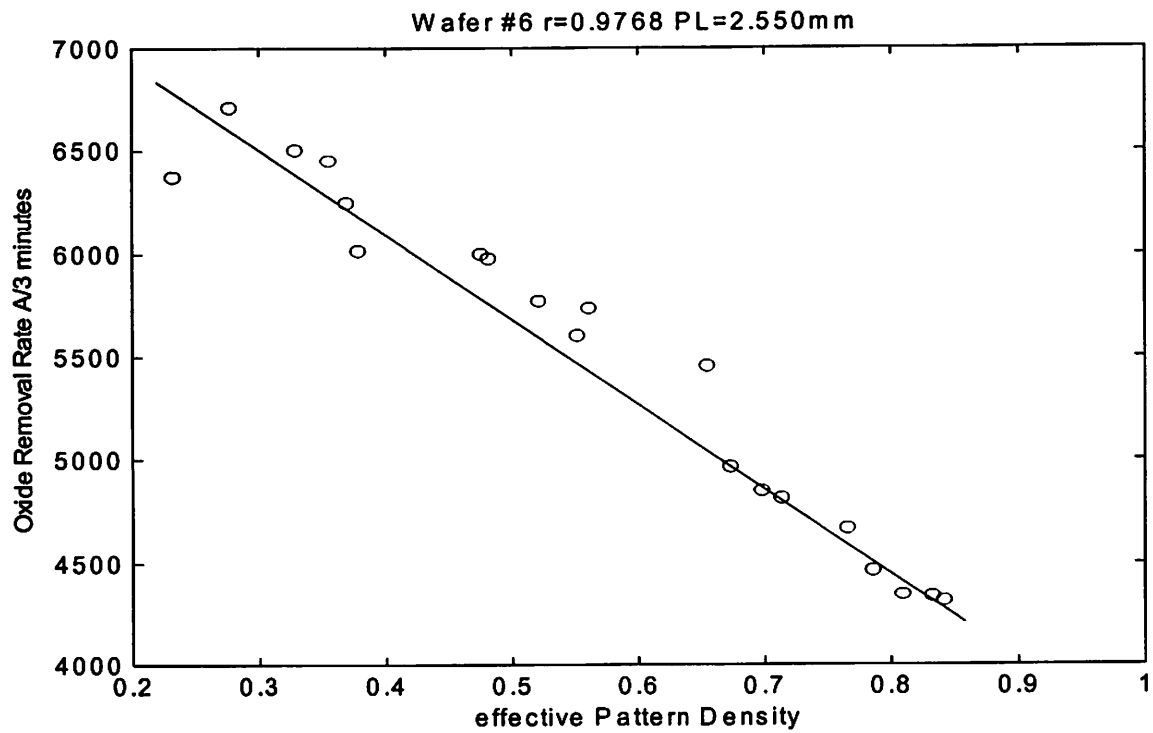
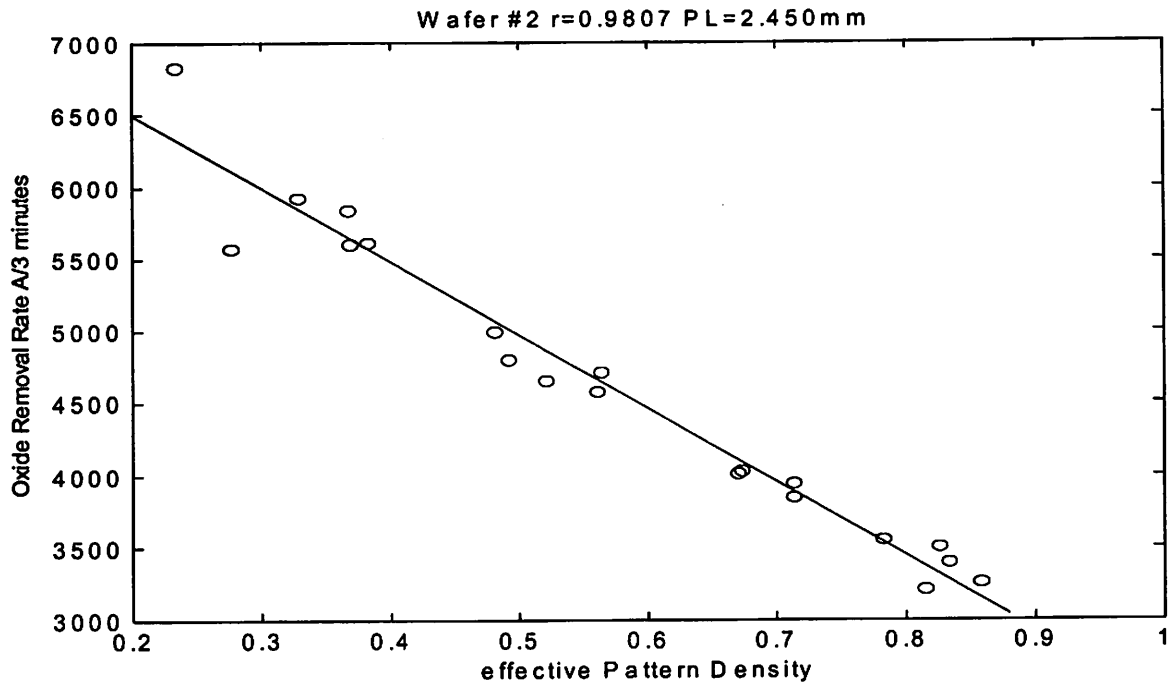


Figure 3.7 Fitted linear regression curve and the extracted planarization length

The fitting was done in order to find the best linear relationship between the effective pattern density and the final oxide thickness. In addition to a strong proportionality between the two variables, we also found that the extracted window size, i.e., the planarization length, is about 2.5-3mm for our system. This tells us that the original MIT pattern density mask is too small to decouple the interactions from the neighboring cells.

This motivated us for our new mask design in order to characterize the oxide CMP process, which is described in detail in the next chapter.

Chapter 4

Enabling Full-Profile CMP Metrology

Using Scatterometry

The general goal of our project is to build a rigorous CMP model by including the appropriate hydrodynamic phenomena and chemical effects to the current simplified CMP model. The specific innovation that goes beyond existing literature is the inclusion of chemical and hydrodynamic effects to the evolution of arbitrary profiles in the sub-micrometer range. As we discussed in the last chapter, the MIT 96.4 pattern density mask did not provide enough pattern density isolation between the various areas.

4.1 Mask Design

In order to achieve the goals mentioned above, motivated by the characterization length extracted from the experiments, we designed our new mask as shown in Figure 4.1.

The first feature of this mask is its enlarged size. In this mask, the pattern density was defined as the ratio of raised area in each structure to the total area of each structure. It was varied systematically from 4% to 100% from lowest in the lower left corner to

greatest in the upper right corner while the pitch of each structure was fixed at $250\mu\text{m}$. A total of 25 structures each $10\text{mm} \times 10\text{mm}$ are arranged in a 5×5 grid fashion. Each block size is $10\text{mm} \times 10\text{mm}$ to minimize interactions from neighboring structures. The second feature of the design is that at the center of each cell we added some gratings for scatterometry metrology. The feature size of the gratings is $1\mu\text{m}$, which is smaller than the minimum feature that could be printed using the Karl Suss MA6 Mask Aligner, top and bottom side contact printer used for fine line lithography down to $2\mu\text{m}$. The process flow will be discussed later in section 4.2.

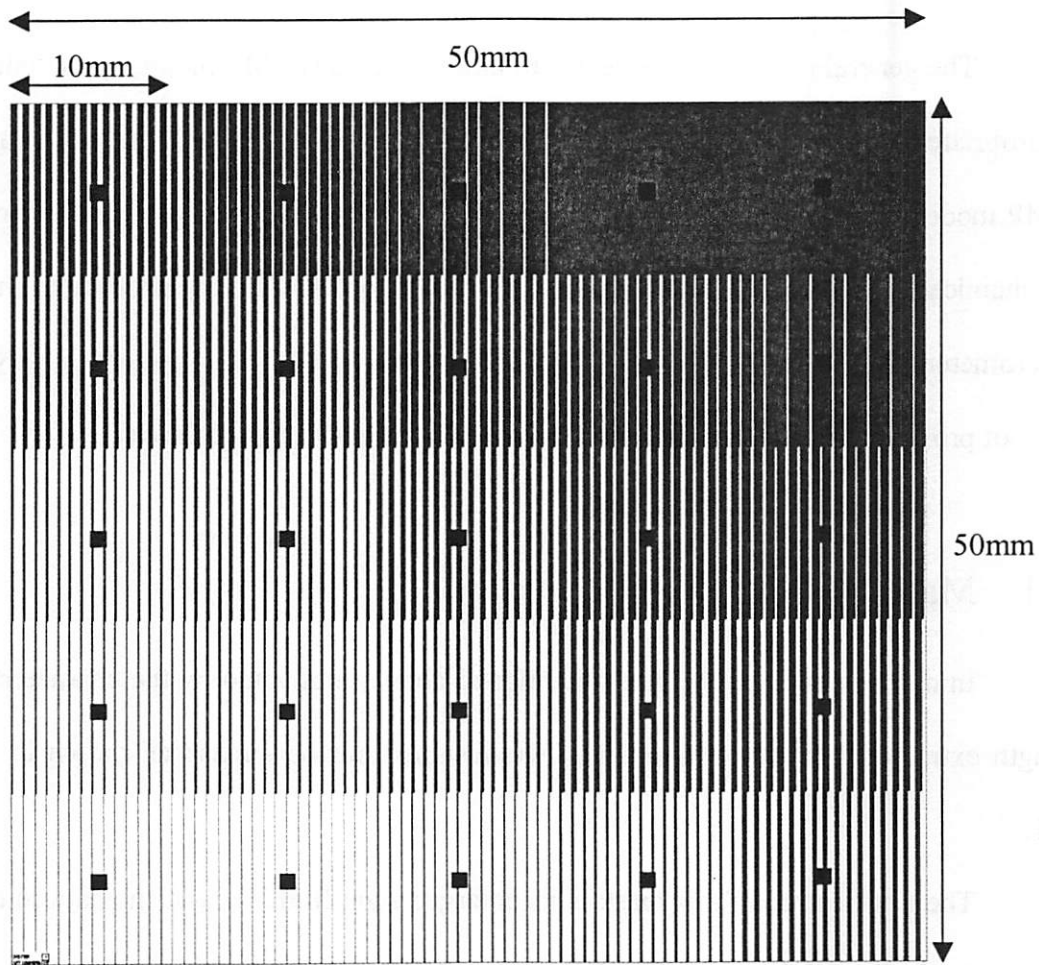


Figure 4.1 The Berkeley 2000.4 CMP characterization mask design

The metrology cell is $250\mu\text{m}$ by $250\mu\text{m}$ size. The pattern density was fixed at 50%, that is, $1\mu\text{m}$ line with $1\mu\text{m}$ space. An important consideration was that the scatterometry cells must be small, so that the polishing rates around them would be mostly determined by the fixed pattern density in the surrounding 10mm square. In order for scatterometry to get a good signal, at least 30 periodic gratings will be needed. The spot size of the scatterometry beam is about $200\mu\text{m}$ in diameter. Figure 4.2 shows the top view of the metrology cell structure.

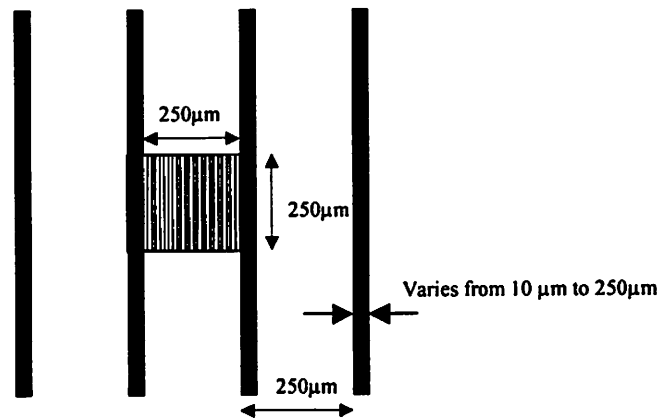


Figure 4.2 Top view of the metrology cell (red structure)

4.2 Key Ideas

Figure 4.3 illustrates the idea of using scatterometry for monitoring CMP profiles. After we polish the oxide layer for a short period of time, use scatterometry to take responses and extract the oxide profiles based on the information available.

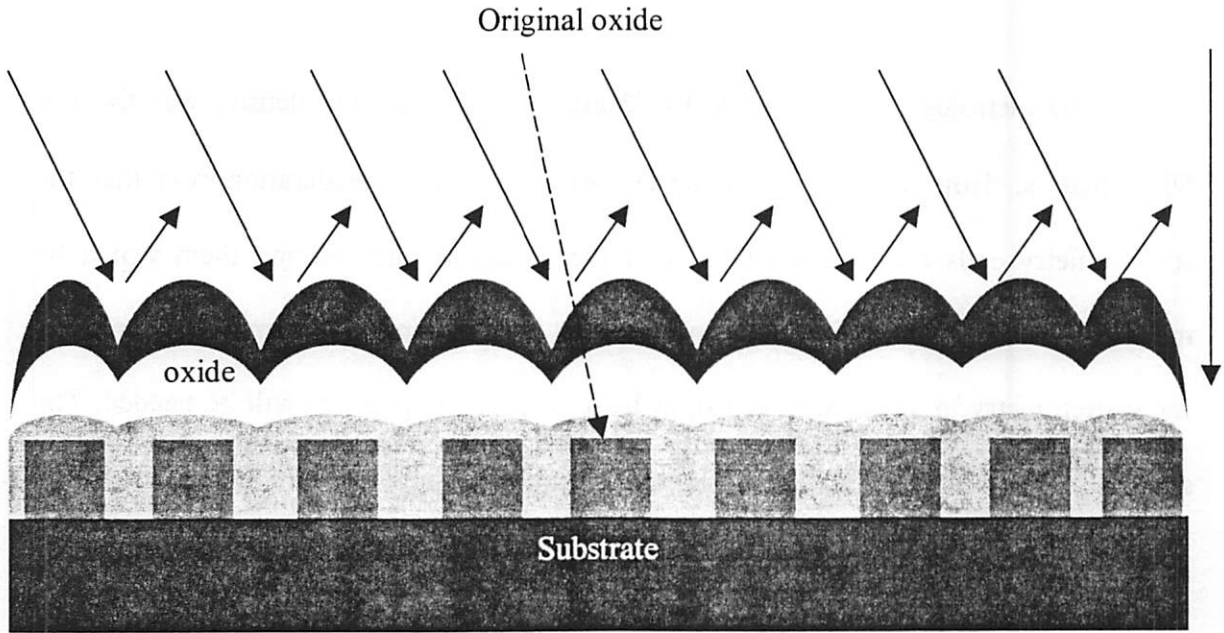


Figure 4.3 Illustration of the key idea of full profile CMP metrology

4.3 Fabrication issues

The process flow was similar to that in Chapter 3, with two exceptions: first, in this fabrication process, we used two masks to pattern the “metal” layer. One is a contact print mask used for patterning wide lines in the 25 10mm×10mm cells. At the center of each cell, we leave a 252μm×252μm die of unexposed photoresist. With a 50% development, the next lithography step could get reasonable alignment. The wafers were next patterned in the stepper to print the fine 250μm by 250μm metrology features on the leftover photoresist, and then the remaining resist was developed; The second difference is that in this process we used a dummy oxide layer to substitute the Aluminum metal layer in Chapter 3. The reason is that the scatterometry signals from the metal would be too strong for us to get any real information about the oxide profile.

4.3 Preparation for the Experiment

Two major issues were addressed before the actual characterization experiments.

First, we understand that in order to verify the functionality of scatterometry on monitoring the CMP oxide profile evolution, a reliable reference tool was highly desirable. With the help of AMD, we got access to the AFM in their sub-micron development center. Four new $0.25\mu\text{m}$ CD tips were bought from Veeco, and were calibrated before we took the measurements.

Next, a simulation was done using the *gtk* tool developed by X. Niu [5]. *gtk* is a software package used to simulate the scatterometry response on periodic gratings. The simulation was on a conceptual oxide profile evolution listed in Figure 4.4. The step height changed gradually from 500nm to 0nm (i.e. a flat surface). The simulated $Tan\Psi$ and $Cos\Delta$ values were listed in Figure 4.5 and Figure 4.6. As we can see, the differences were quite strong, and should be detectable.

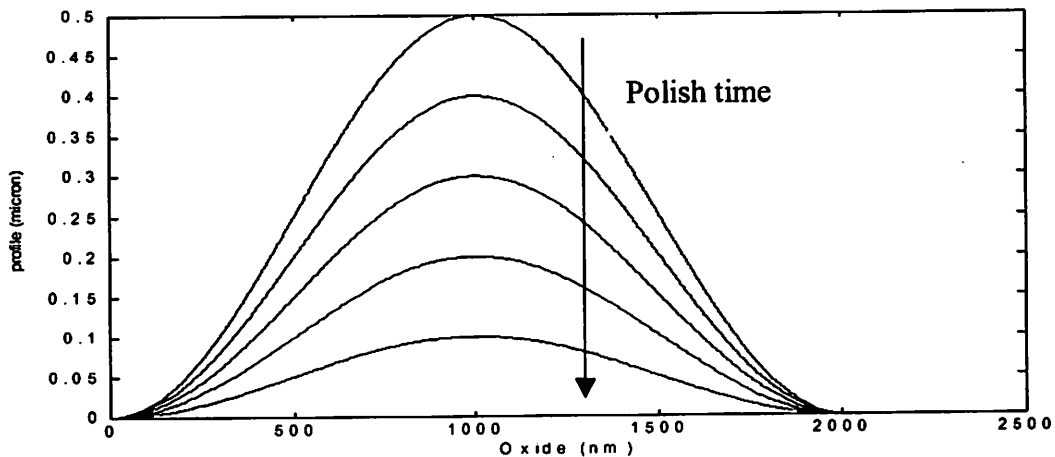


Figure 4.4 Oxide profile evolution used in the *gtk* simulation

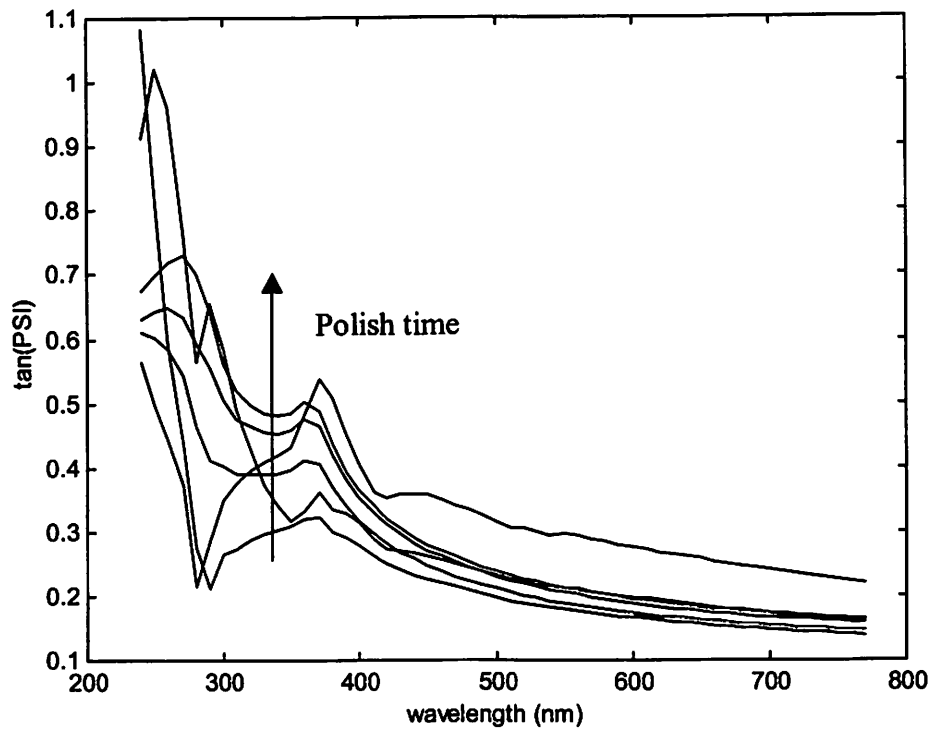


Figure 4.5 $\tan\Psi$ response variation due to profile evolution

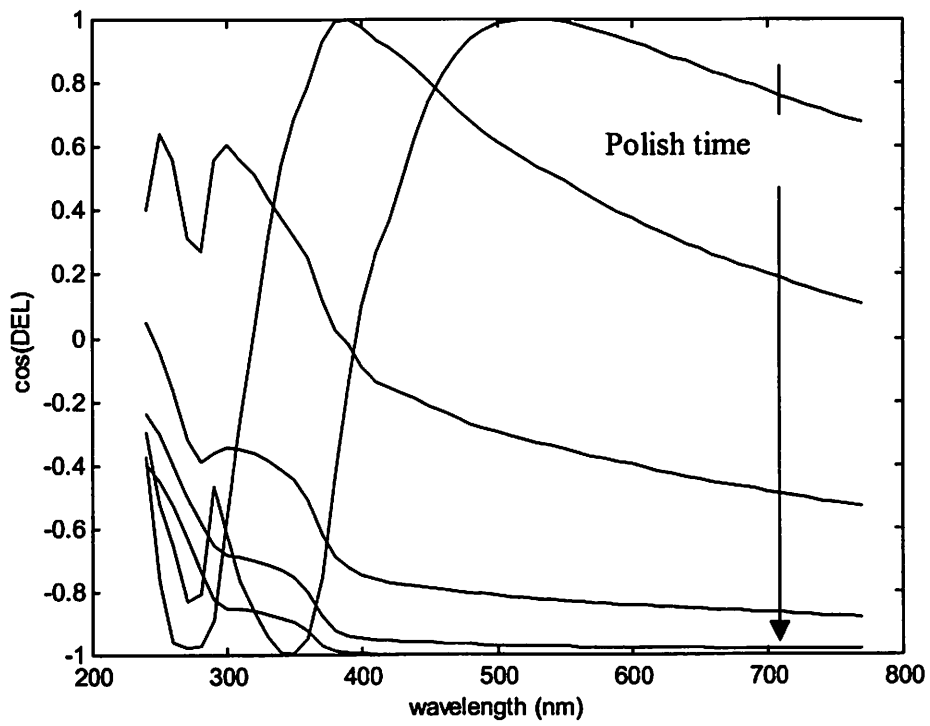


Figure 4.6 $\cos\Delta$ response variation due to profile evolution

4.4 Experiments

As we mentioned in the previous section, two masks and a double exposure technique were used to fabricate the wafers. A top view and a cross-sectional view of the final structure were shown in Figure 4.7, where the dark cells contain the periodic scatterometry gratings.

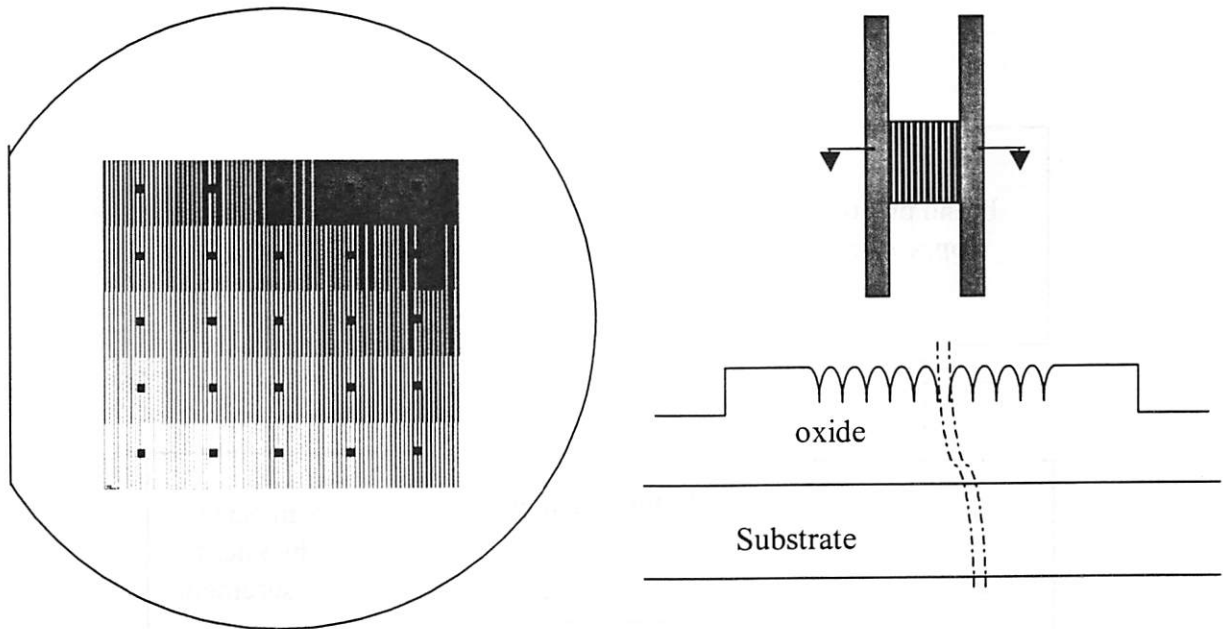


Figure 4.7 Top and cross-sectional view of the final structure before CMP

In the original Strausbaugh 6EC system, for a planar oxide on silicon wafer, the post polishing non-uniformity could be as high as 30%. The pad and ring of the polisher were changed before the experiments in order to mitigate the non-uniformity problem. ~10% non-uniformity was achieved after the upgrade.

Additionally, the oxide thickness measurement tool - Nanometrics 210 XP Scanning UV Microspectrophotometer (Nanospec) and the Sopra GESP broadband

variable angle scatterometry (Sopra) were both carefully calibrated before the experiments.

Table 4.1 shows the values of different parameters that were used in the design of experiments. Figure 4.8 helps explain the iteration of experiment flow. Totally three one-minute iteration polishing steps were finished in this experiment, using the parameters listed in Table 4.1.

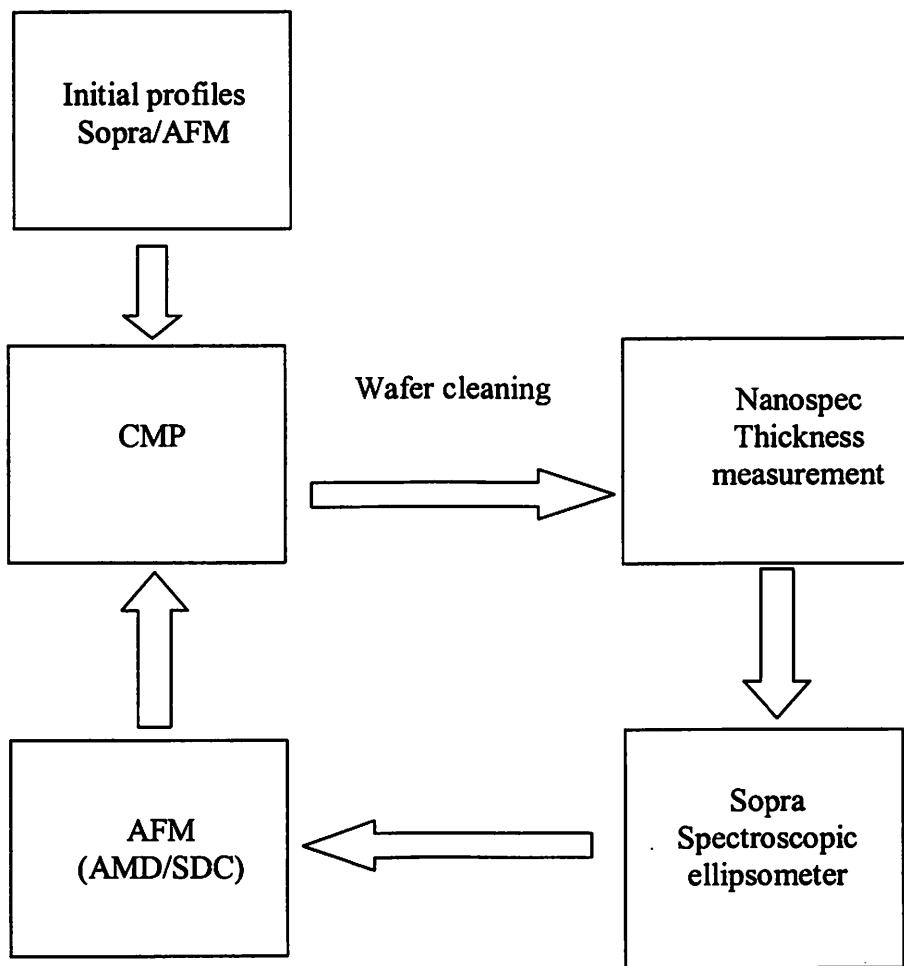


Figure 4.8 Iteration steps in the CMP characterization experiments

Table 4.1 Factorial designs of experiments

Wafer #	Down Force (psi)	Table Speed (rpm)	Slurry Flow (ml/min)
1	4	40	50
2	8	40	50
3	4	40	150
4	8	40	150
5	8	80	50
6	4	80	50
7	8	80	150
8	4	80	150
9	6	60	100
10	6	60	100
11	6	60	100

4.5 Measurements

Thickness information will be useful in both the factorial analysis and in building the response library. We took four measurements on each corner of the metrology cell (as shown in Figure 4.9). By averaging the four measurements the thickness (total height) of the oxide layer were calculated. Figure 4.10 shows that this method is a good approximation to the real topography on the local wafer surface. This AFM profile measurement shows that the top of the wide line was almost that of the small lines used in the scatterometry measurements.

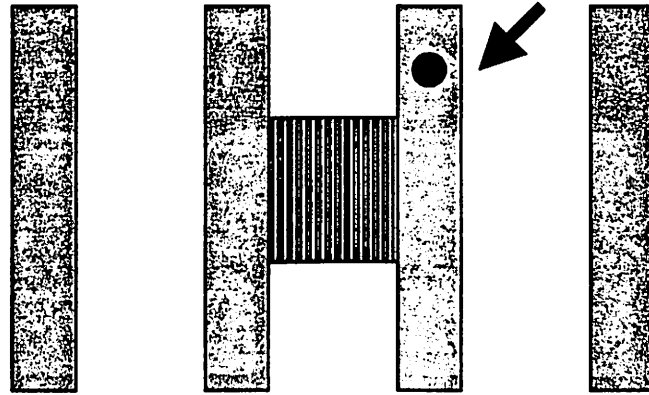


Figure 4.9 Nanospec measurements on the neighboring wide line of the metrology cell

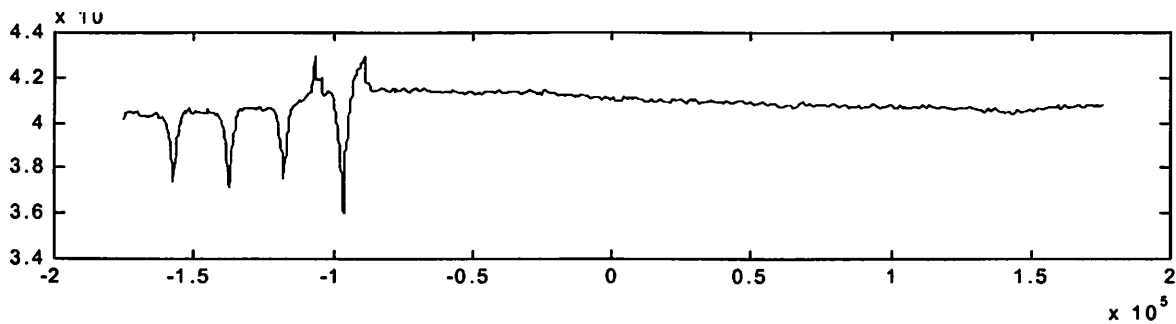


Figure 4.10 AFM measurement on the metrology cell and the neighboring wide line

Another important issue was the cost of the measurements. Since each Sopra measurement took approximately 10 minutes, 11 wafers with 25 points on each wafer would take 2750 minutes = 45.83 hours = 6 workdays for each round of polishing! For 3 rounds it would take about a month to do the scatterometry measurements. Sopra is not an automated system and everything requires manual operation, especially wafer alignment after the measurement on each cell. So we decided to take fewer points as shown in Table 4.2 (cells in bold format).

Table 4.2 Measurements taken in the experiments

60%	76%	88%	96%	100%
40%	56%	72%	84%	92%
24%	36%	52%	68%	80%
12%	20%	32%	48%	64%
4%	8%	16%	28%	44%

As shown, the five points on each wafer were measured. They correspond to 20%, 36%, 52%, 68% and 84% pattern density, respectively.

The wafers were then transferred to AMD at Sunnyvale and AFM measurements were taken after each round of polishing. We did three one-minute polishing steps in total.

The metrology information obtained in this step will be further discussed in the following sections 4.6 and 4.7.

4.6 Factorial Data Analysis

The idea of factorial design and factorial analysis can be shown in Figure 4.11 [13]. This technique uses a few runs to maximize the value of the data. Factorial designs can achieve economy in experimentation.

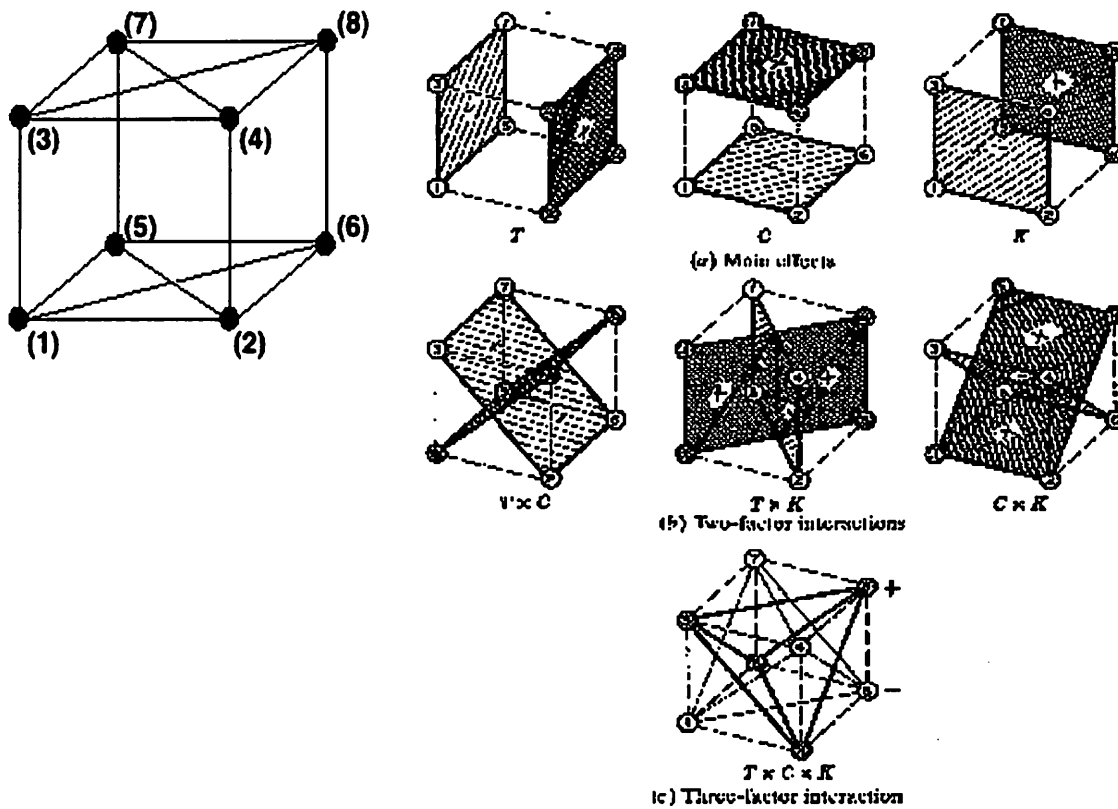


Figure 4.11 Illustration of factorial design (left) and factorial analysis (right)

In this two level factorial CMP experiment design, the down force (D) was 4-8psi, table speed (T) 40-80rpm, slurry flow (S) 50-150ml/min. The removal rate was in A/min, so the factorial analysis results were listed in the following table 4.2.

Table 4.2 factorial analysis of different effects and their significance

D T S	R	Effects	
- - -	1913.6	AVG	2719.8
- - +	1054.2	D	-1230.4
- + -	3483.4	T	2745.9
- + +	6889.2	S	460.3
+ - -	1560.4	DT	-956.4
+ - +	859.4	DS	-812.8
+ + -	3001.4	TS	1240.5
+ + +	2997.4	DTS	-892.0

To estimate the noise level in the experiments, we assume that there was no significant effect, that is, any change we observed was due to randomness. The standard deviation of the data was 1940.3Å/min. Under this context, we see that Table speed (T) was the only significant effect factor from this experiment. The down force (D) was not examined as a significant factor in this experiment, most likely due to the bad pressure range we chose. As listed in J. Luo’s paper [9] pressure has a non-linear effect on the material removal rate. If the range chosen was around the transitional area, this effect might be overwhelmed by the wafer-to-wafer removal rate variations.

Another analysis is the round to round comparison of the removal rate. As shown in Figure 4.12, the results in two rounds were highly correlated. The diamond light line

stands for the removal rate in the first round for different points (the horizontal axis) while the square line stands for that in the second round. For this figure we can also see that the material removal has a step-height dependency: in this case, the larger the step height, the higher the removal rate.

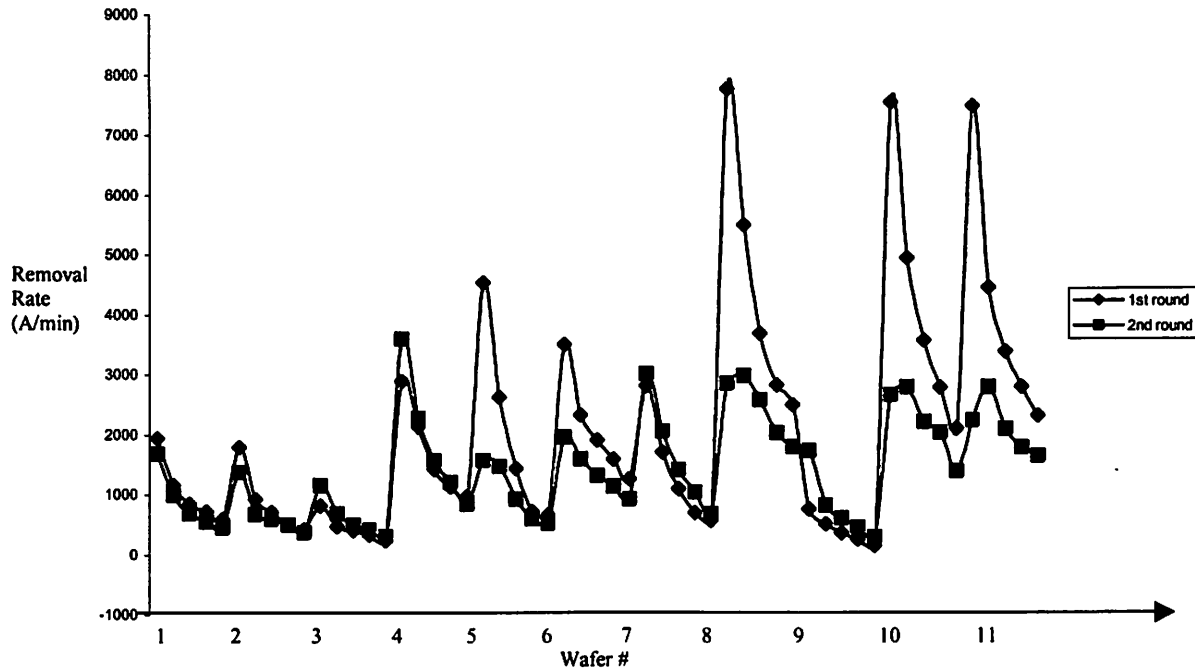


Figure 4.12 Round to round removal rate comparison

The last analysis was on the pattern density dependency. Here the material removal rates for different pattern densities is shown in Figures 4.13 and 4.14, where the first shows all 11 different wafers while the latter depicts the average removal rate of the 11 wafers. In Figure 4.14, the R^2 is 0.989 for the linear fitting, a very good fit, considering the fact that the CMP system only had ~10% non-uniformity level for unpatterned wafers.

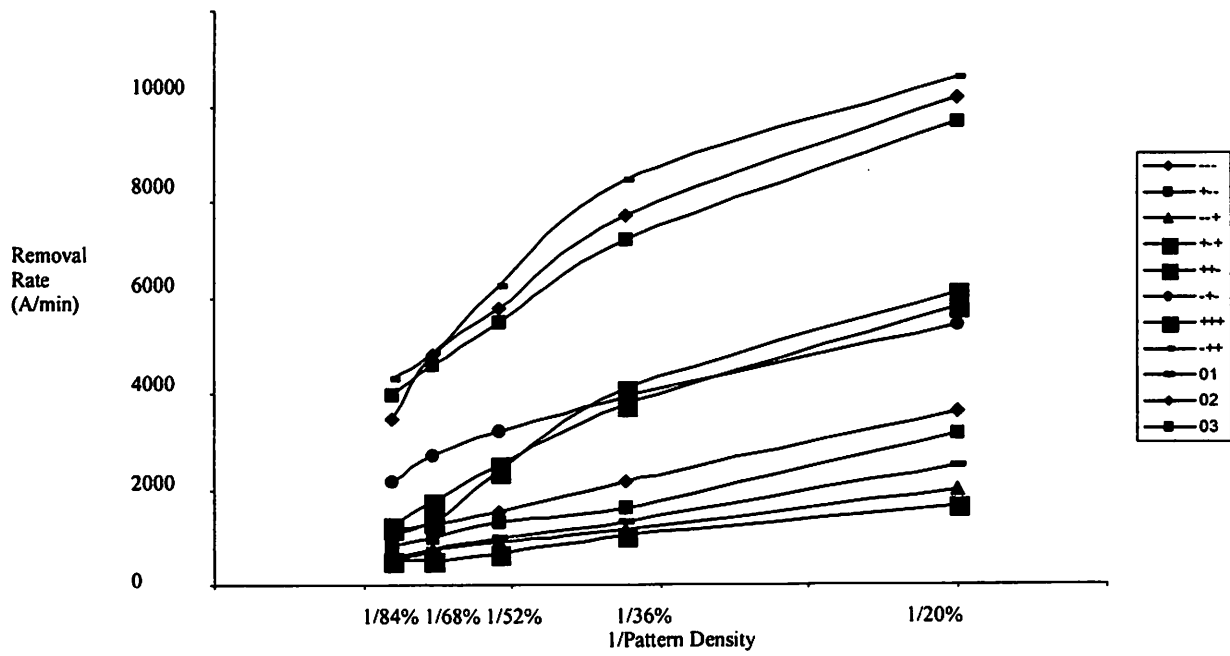


Figure 4.13 Polish rate for different pattern densities (11 wafers)

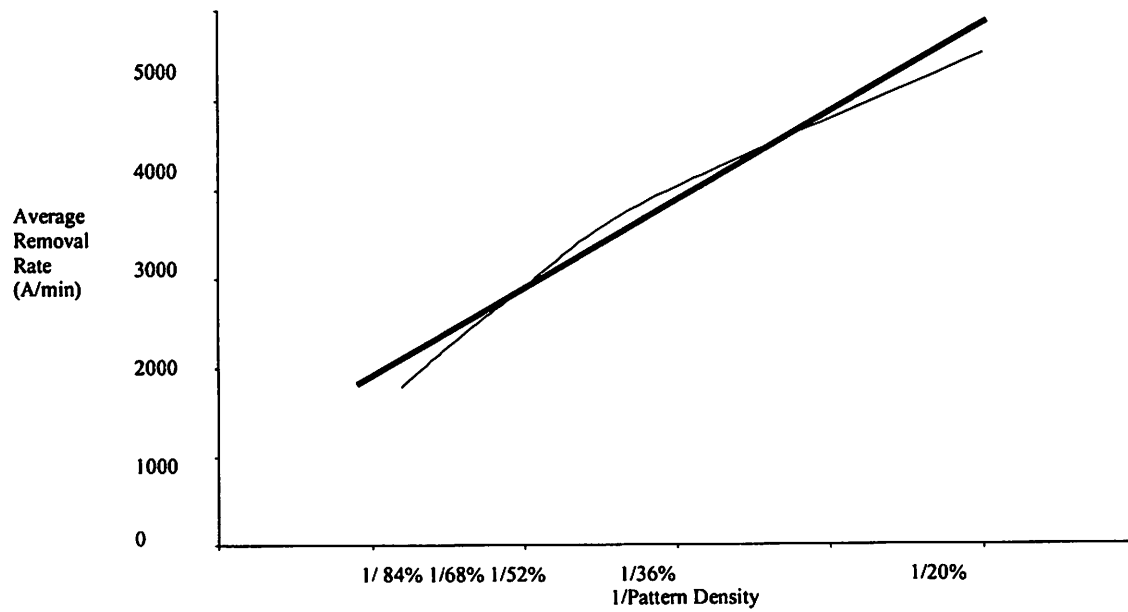


Figure 4.14 Linear pattern density dependency

4.7 A library-based metrology for monitoring CMP profile evolution

The application of measurements on IC wafers by diffraction from grating test patterns has been pursued for quite a few years [14]. X. Niu presented an integrated metrology system in DUV lithography system in 1999 [5]. The idea of a library is that we pre-simulate the scatterometry responses for hundreds of thousands profiles and organize them as a library. A fast search algorithm is subsequently needed to search the library to get the closest response. So the minimum error match can be extracted, hence we can get the needed profile information. Figure 4.15 illustrates this idea.

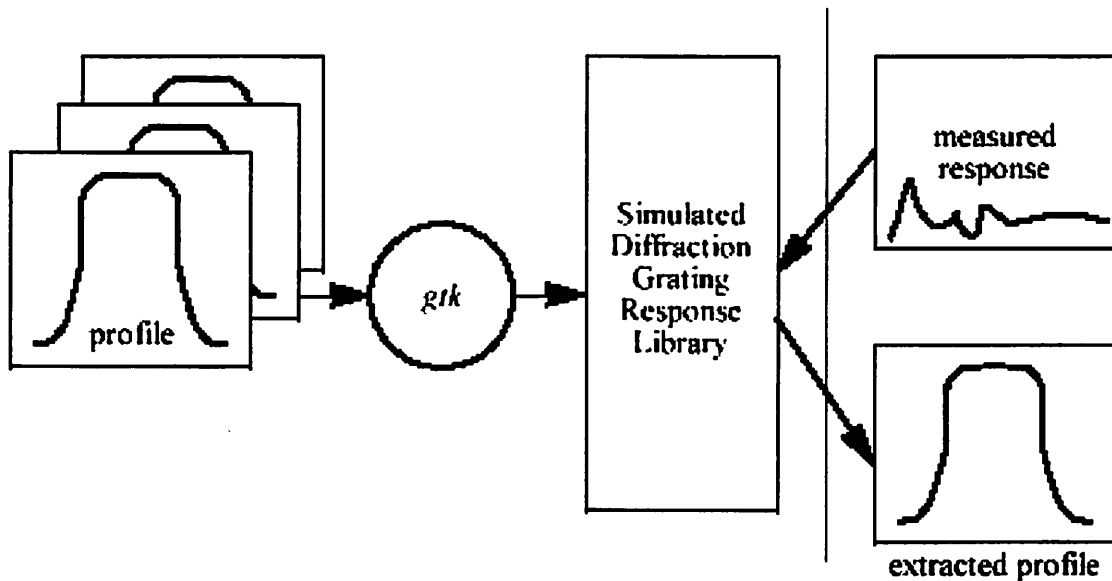


Figure 4.15 Library-based CD profile extraction

A spectroscopic ellipsometer (Sopra) was used in this work for 1D gratings. With this configuration, the ratio of the 0th order complex transverse electric (TE) and transverse magnetic (TM) reflectivity is measured, where is the 0th order TM reflectance coefficient and is the 0th order TE reflectance coefficient.

The extraction of the oxide CMP evolution profile can be viewed as an optimization problem [15-16]. The objective is to find a profile whose simulated diffraction responses match the measured responses.

In this experiment, the process flow for monitoring CMP profile evolution is as follows:

First, thin-film information (optical properties, and thickness values), are used to obtain a collection of profiles. The profile information includes the information of the grating layer and all the underneath layers (in this case, it's just LTO oxide). The profiles can be obtained by a random profile generator or in this case, a method using a few descriptive parameters varying within certain range. Five variables were used in the oxide

CMP profile library: Bottom height (A), Bottom width (B), Slope 1 (C), Slope 2 (D) and Top oxide height (E).

Second, the profiles are used as inputs to a diffraction grating simulator *gtk*, to generate the simulated diffraction responses; they are simulated over a wide range of wavelengths (240nm to 760nm).

Third, the diffraction responses are measured and compared with the library. When the process is complete, there will be one or more profiles

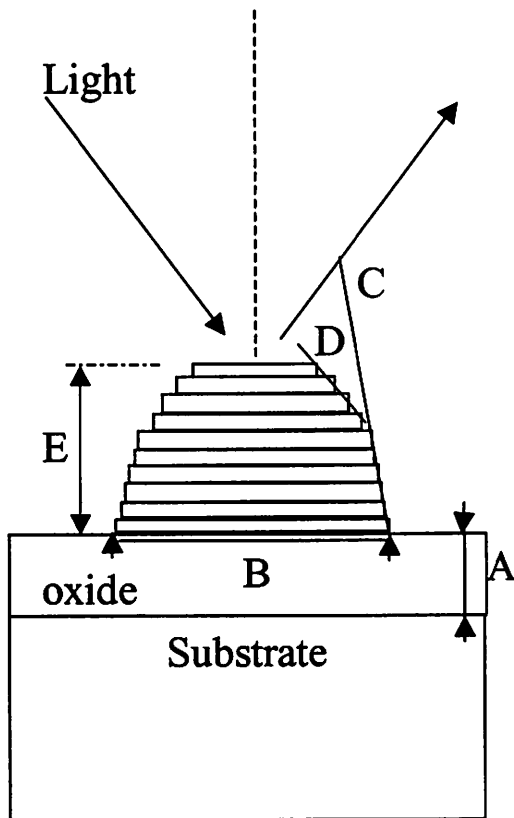


Figure 4.16 Profile description parameters

whose simulated responses match those of the measured sample.

The key of the success for this library-based extraction methodology is the completeness of the library combined with efficient search methods. One challenge for the CMP oxide profile extraction is that the thickness covers a long range (from 1200nm to 0nm).

After simulating the same structure at different orders, it was determined to use 15 TE and 15 TM orders in the RCWA simulation since Figure 4.17 shows that there is very little difference between 15 orders and 20 orders. To save simulation time, fewer orders were retained because simulation time is approximately proportional to the square of the order used in the simulation.

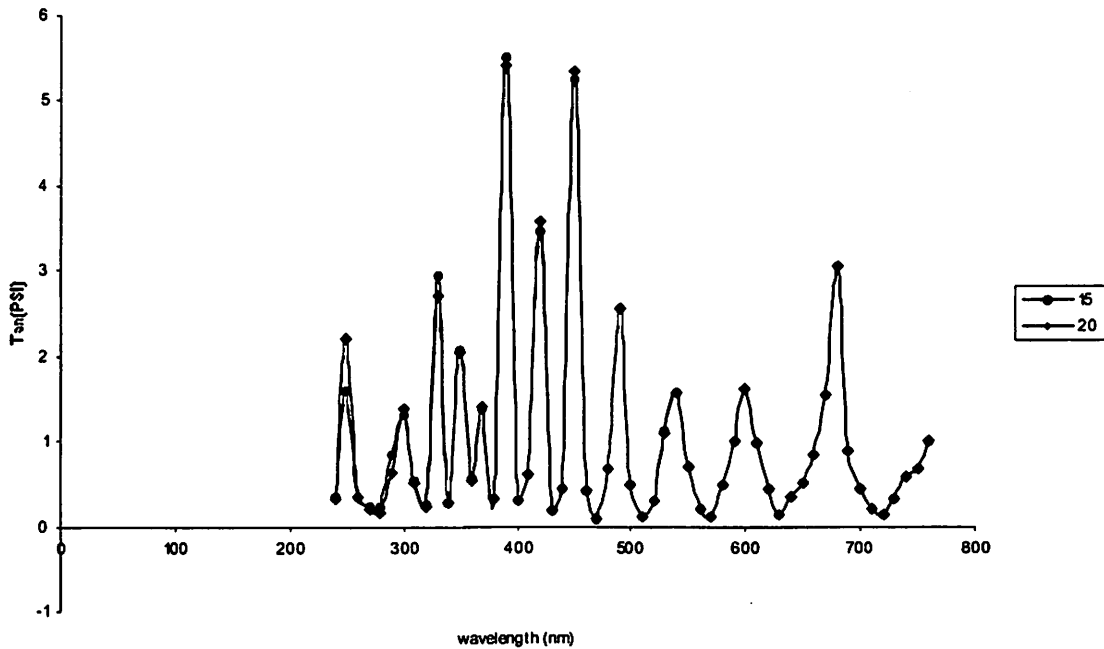


Figure 4.17 Scatterometry response vs. the order retained in RCWA

To verify the effectiveness of this method, we used the AFM to measure the profiles and used SEM to get a cross-sectional view of the gratings. The AFM, SEM measurements and the extracted profiles were shown in Figures 4.18, 4.19, 4.20, respectively.

As we can see, the extracted profile evolution using this library-based scatterometry has a good match with that of the SEM. AFM, since its CD-tip head dimension is about 200nm, could not go down to the bottom features hence could only provide the profile evolution at the top part. We can conclude that although cross-sectional SEM and AFM can deliver direct images of small structures, they are expensive, and can be either time-consuming or destructive. Scatterometry can extract the profile in less than one second for a library with 10,000 profiles with a precision of 10nm. It takes about 10 days to build the library using a 500Mhz PC with 128M DRAM.

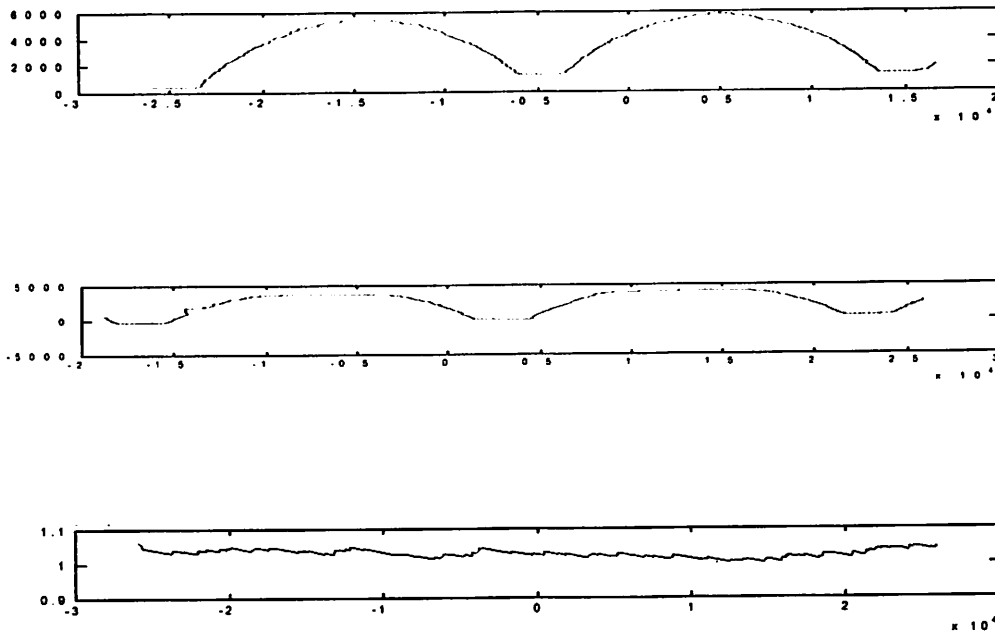


Figure 4.18 Oxide CMP Profile evolution monitoring using AFM

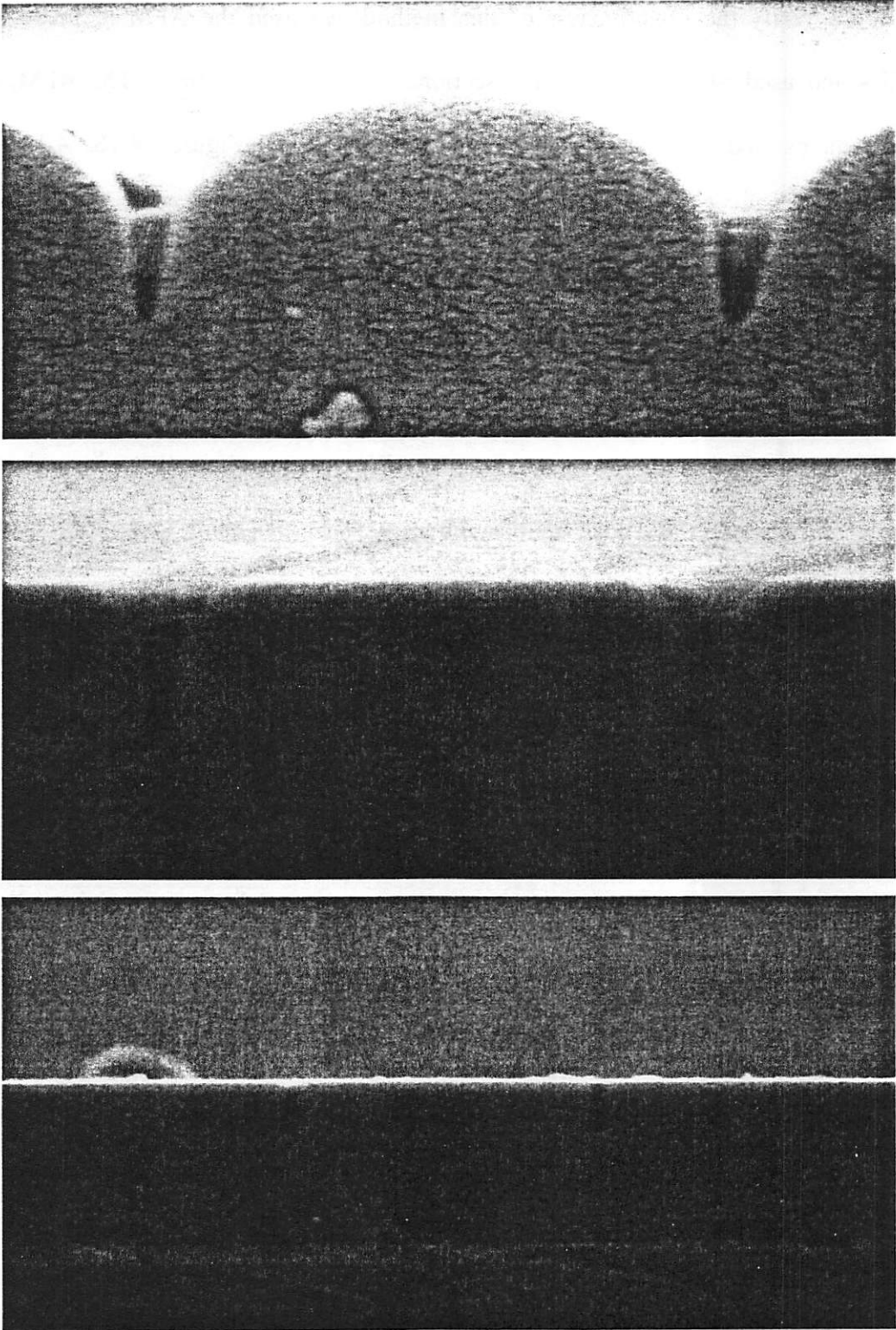


Figure 4.19 Oxide CMP profile evolution using SEM

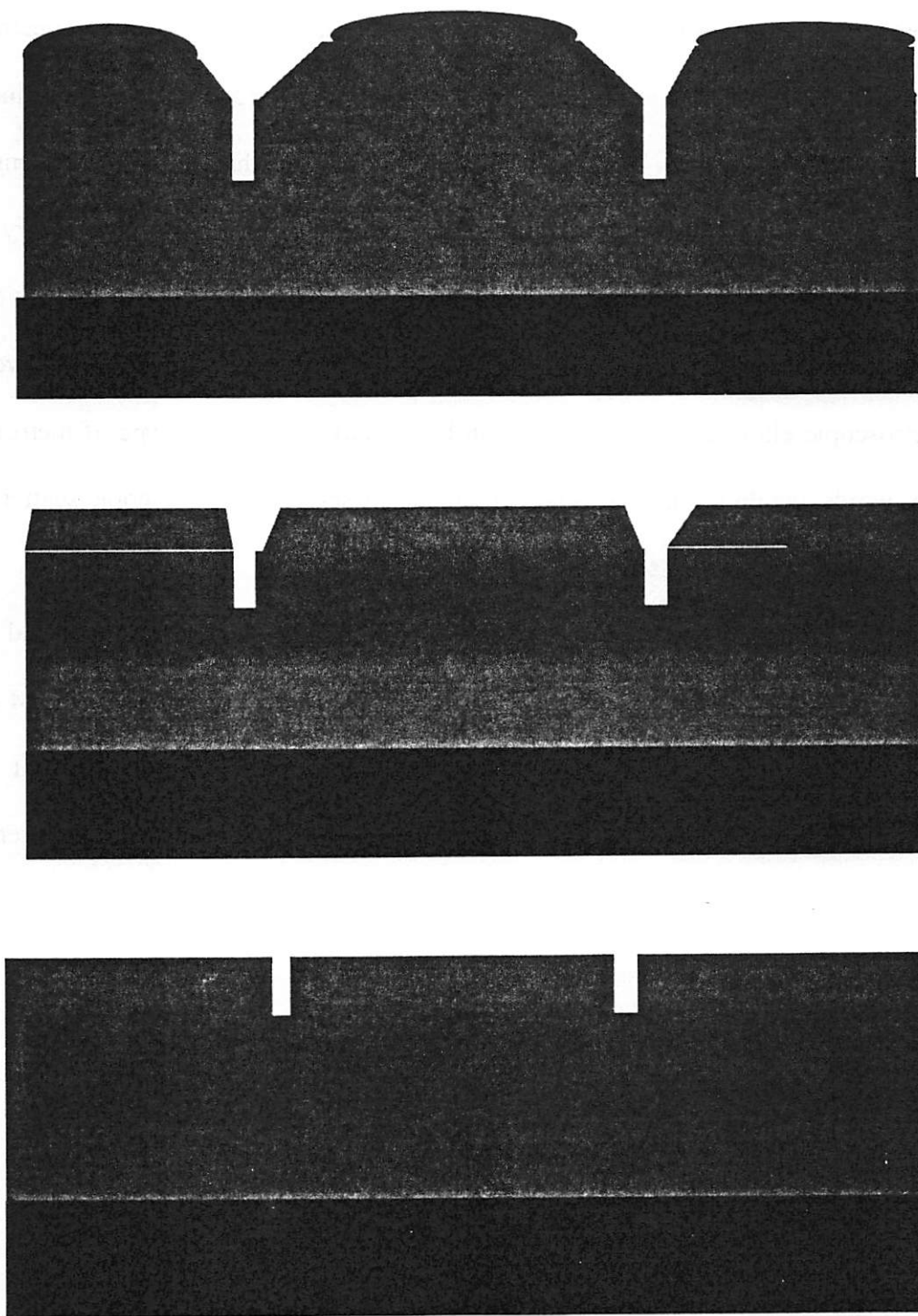


Figure 4.20 Extracted oxide CMP profile evolution using Library-based scatterometry

Scatterometry is one of the few metrology candidates that have true *in-situ* potential for deep sub-micron oxide CMP profile analysis. The specular spectroscopic scatterometry is designed to measure the 0th diffraction order at a fixed angle of incidence and multiple wavelengths. The term “spectroscopic” means that multiple wavelengths are under consideration. Due to its fixed angle, specular spectroscopic scatterometry is easy to deploy. Specular spectroscopic scatterometry can make use of a conventional spectroscopic ellipsometer, and can be easily installed *in-line or in-situ*. Conventional spectroscopic ellipsometry equipment can be directly used in this type of metrology. In other words, we do not need special equipment for specular spectroscopic scatterometry, as the cost of hardware is shifted to software.

In summary, specular spectroscopic scatterometry, when implemented with a library of generated profiles, is about a factor of 100 times faster than the SEM and the speed advantage is even more significant when compared with the AFM. It is non-destructive, inexpensive and easy to implement *in-line* in a production CMP system.

Chapter 5

Conclusions and Future Work

5.1 Report Summary

Moore's Law predicts the exponential scaling factor for integrated circuit density [17]. However, this aggressive scaling relies on an effective and reliable planarization process on ILD and metal layers. Advanced CMP process modeling and affordable CMP metrology at and below 150nm now become the next big challenge. This report has presented some experimental and analytical attempts for measuring and modeling of patterned oxide wafers in the CMP process. In Chapter 3, the characterization experiment using the MIT pattern density mask is conducted. The linear pattern density dependency was verified and the extracted results motivated us a new mask design. In chapter 4, the process with the new mask integrating some scatterometry metrology structures was designed and materialized. A statistical design of experiments was proposed, the data were primarily analyzed to explore the effect of different process parameters. More importantly, with the ability to simulate the behavior of diffraction gratings with high precision, we proposed and verified a library-based full-profile CMP metrology using specular spectroscopic scatterometry. This method is cost effective, non-destructive and much faster than the traditional methods such as SEM and AFM.

5.2 Future Work

The main purpose of this project is that, through the aid of computation and fast data analysis techniques, more process information can be extracted from the poorly understood CMP process. This information can be used for process modeling and design improvement. With the assistance of specular spectroscopic scatterometry, it is expected that the *in-situ or in-line* metrology of CMP profile can become realistic. At the same time, the use of profile information for small feature CMP modeling becomes a compelling research topic.

References

- [1] "International Technology Roadmap for Semiconductors", 1999 Edition, Semiconductor Industry Association (SIA).
- [2] <http://www.semiconductor.net/semiconductor/reference/reference.asp> "Editorial Archives", May 2001.
- [3] C. J. Raymond, S. S. H. Naqvi, J. R. McNeil, "Scatterometry for CD measurements of etched structures," Proceedings of SPIE, vol. 2725, 720-728, March 1996.
- [4] X. Niu, N. Jakatdar, J. Bao, C. Spanos, S. Yedur, "Specular spectroscopic scatterometry in DUV lithography", Proceedings of the SPIE - The International Society for Optical Engineering, vol.3677, pt.1-2, (Metrology, Inspection, and Process Control for Microlithography XIII, Santa Clara, CA, USA, 15-18 March 1999.
- [5] X. Niu, "An Integrated System of Optical Metrology for Deep Sub-Micron Lithography", Ph.D Dissertation, U.C. Berkeley, 1999.
- [6] X. Niu, N. Jakatdar, J. Bao and C. J. Spanos, "Specular Spectroscopic Scatterometry in DUV Lithography", SRC Techcon'98.
- [7] F.W. Preston, "The Theory and Design of Plate Glass Polishing Machine," Journal of the Society of Glass Technology, Vol. 11, pp. 214-256, 1927.
- [8] L.M. Cook, "Chemical Processes in Glass Polishing", J. of Non-Crystalline Solids, vol. 120, pp152-171, 1990
- [9] J. Luo and D.A. Dornfeld, "Material Removal Mechanism in Chemical Mechanical Polishing: Theory and Modeling", IEEE Transactions on Semiconductor Manufacturing, vol. 14, no. 2, May 2001.

- [10] D. O. Ouma, B. Stine, R. Divecha, D. Boning, J. Chung, I. Ali, and M. Islamraja,,
"Using Variation Decomposition Analysis to Determine the Effect of Process on Wafer
and Die-Level Uniformities in CMP," First International Symposium on Chemical
Mechanical Planarization (CMP) in IC Device Manufacturing, Vol. 96-22, pp. 164-175,
190th Electrochemical Society Meeting, San Antonio, TX, Oct. 6-11, 1996.
- [11] Divecha, R., B. Stine, D. Ouma, J. Yoon, D. Boning, J. Chung, O.S. Nakagawa, S-Y
Oh, "Effect of Fine-Line Density and Pitch on Interconnect ILD Thickness Variation in
Oxide CMP Processes," 1997 Chemical Mechanical Polish for ULSI Multilevel
Interconnection Conference (CMP-MIC), p. 29, Santa Clara, February, 1997.
- [12] G. Nanz and L. E. Camilletti, "Modeling of Chemical-Mechanical Polishing: A
Review," *IEEE Trans. Semiconductor Manufacturing*, Vol. 8, No. 4, November 1995.
- [13] D.C. Montgomery, "Introduction to Statistical Quality Control," 2nd Edition, 1991.
- [14] W. A. Bosenberg and H. P. Kleinknecht, "Linewidth measurement on IC wafers
by diffraction from grating test patterns", *Solid State Technology*, vol. 26, 79-85, July
1983.
- [15] D.A. Pierre, "Optimization Theory with Applications," October 1986.
- [16] R.K. Sundaram, "A First Course in Optimization Theory," June 1996.
- [17] G.E. Moore, "The Role of Fairchild in Silicon Technology in the Early Days of
'Silicon Valley'," *Proceedings of the IEEE*, Volume: 86, Issue: 1, pp. 53-62, Jan. 1998.